	Mean intensity	Variance	P-value
Gene	0.182	1.01	
Pseudogene	0.340	1.20	1.3×10^{-4}
Non-coding	0.394	1.55	2.5×10^{-12}

FIG. 3. Distribution of signal intensity in each region. Mean signal intensities of individual regions were calculated, and the ratio against the corresponding total number in the *M. leprae* genome was plotted for genes, pseudogenes, and noncoding regions. Mean signal intensities, variances, and *P* values from Student's *t* test were calculated for the entire region and are shown below the graph.

The distribution of signal intensities among the genes, pseudogenes, and noncoding regions was evaluated by calculating the average intensity of each probe within a single region and plotting the relative values (Fig. 3, upper panel). If hybridization occurred in a random fashion independent of RNA expression levels, the expectation is that all of the probes would exhibit the same distribution of signal intensities among the genes, pseudogenes, and noncoding regions. However, while positive regions were detected in similar proportions in genes, pseudogenes, and noncoding regions, with no difference in the mean lengths of the positive regions among the three groups, the array data showed stronger signal intensities in the noncoding regions (Fig. 3, right shoulder of the graph). The mean intensity in coding genes (0.182) was significantly lower than that in noncoding regions (0.394) ($P = 2.5 \times 10^{-12}$) and pseudogenes (0.340) ($P = 1.3 \times 10^{-4}$) (Fig. 3, lower panel). High RNA expression from a noncoding region (Fig. 2D) suggests that those RNAs have a biological function. However, no sequence homology was identified in these regions after intensive database searches.

A total of 168 positive areas, some spanning more than one region, were found based on the applied criteria (>60% of the maximum level). When an expressed area overlapped two or more annotated genes or noncoding regions, they were counted separately based on each annotation (as shown in Fig. 2B and C). A noncoding region longer than 114 bp, which is the minimum length of an evaluated area, was counted as a single expressed region. As a result, 209 positives from genes, pseudogenes, and noncoding regions were classified as strong expressers. The number from each region, the mean length of

TABLE 1. Numbers of highly expressed genes, pseudogenes, and noncoding regions identified by tiled microarray analysis

Genetic material	No. identified	% of total	Mean length (bp)	Mean peak intensity[a]
Genes	63	30.1	637	4.88
Pseudogenes	78	37.3	611	5.11*
Noncoding regions	68	32.5	634	5.38**
Total	209	100		

[a] Mean peak intensities of pseudogenes and noncoding regions were statistically compared with the intensity of coding genes (*, $P < 0.05$; **, $P < 0.00001$ by Student's *t* test).

the positive regions, and the mean peak signal intensities are summarized in Table 1.

Functional classification of expressed genes and pseudogenes. Gene expression profiles obtained from tiling array analysis were classified based on criteria that were originally determined during whole-genome sequence analysis of *M. tuberculosis* (4) and later applied to *M. leprae* (5) (Table 2). Among genes, the "cell processes" class (constituting genes with functions such as transport, secretion, and chaperone function) was highly expressed (9.8%) compared to genes overall (3.9%) ($\chi^2 = 7.1$, $P = 0.008$). Among the "small-molecule metabolism" class, the "amino acid biosynthesis" (4 out of 77) and "purines, pyrimidines, nucleosides, and nucleotides" (4 out of 52) subsets were highly expressed, while expression of the "biosynthesis of cofactors, prosthetic groups, and carriers" subset was not observed (0 out of 63). Similarly, in the "macromolecule metabolism" class, the "cell envelope" subset was expressed (13 out of 256), but the "degradation of macromolecules" subset was not (0 out of 43) ($\chi^2 = 2.8$, $P = 0.251$). Three out of 11 PE and PPE protein gene families found in the "other functions" class were expressed among the coding genes.

Pseudogenes were classified based on criteria defined by the function of their counterpart genes (5) (Table 2). Pseudogene expression was significantly higher in the "other functions" class than in other classes ($\chi^2 = 40.9$, $P = 1.00 \times 10^{-7}$). No significance was detected when this class was excluded ($\chi^2 = 1.7$, $P = 0.793$). In the "other functions" class, 15 expressed

TABLE 2. Numbers and percentage of expressed genes and pseudogenes based on functional classification[a]

Gene function/type	No. of expressed genes or pseudogenes/total no. of genes or pseudogenes (%)	
	Genes	Pseudogenes
Small-molecule metabolism[b]	19/467 (4.1)	19/334 (5.7)
Macromolecule metabolism[c]	16/458 (3.5)	10/163 (6.1)
Cell processes[d]	10/102 (9.8)	2/67 (3.0)
Other functions[e]	6/77 (7.8)	29/133 (21.8)
Conserved hypotheticals	6/360 (1.7)	18/416 (4.3)
Unknowns	6/141 (4.3)	0/2 (0)
Total	63/1,605 (3.9)	78/1,115 (7.0)

[a] Functional classification per references 4 and 5.
[b] Synthesis and degradation of amino acid, polyamine, nucleotide, cofactor and lipid, and energy metabolism enzymes.
[c] Synthesis and degradation of protein, RNA, DNA, and cell envelope.
[d] Transporter and chaperone.
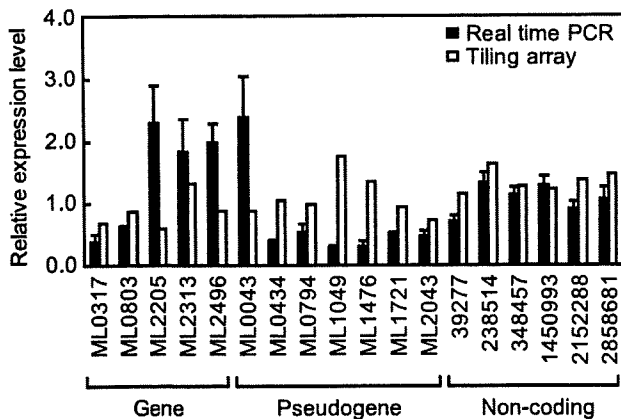[e] Virulence, repeated sequence, and PE and PPE families.

FIG. 4. Comparison of RNA expression between real-time PCR and tiling array. Relative RNA expression levels detected by tiling array analysis and quantitative real-time PCR were compared. Genes and pseudogenes are indicated by accession numbers. Noncoding regions are indicated by their starting position in the *M. leprae* genome. Data are from three independent real-time PCRs and are expressed as means ± standard errors.

pseudogenes contained parts of the LEPREP repeat sequence. Markedly expressed pseudogenes were also found in the "degradation" (5 out of 74) and "energy metabolism" (7 out of 118) subsets of the "small-molecule metabolism" class, although the expression was not statistically significant among pseudogenes (78 out of 1,115). The overall expression level of pseudogenes (7.0%) was higher than that of genes (3.9%) ($\chi^2 = 11.3$, $P = 0.001$). However, the "cell processes" class showed significantly higher gene expression (9.8%) than pseudogene expression (3.0%) ($\chi^2 = 6.6$, $P = 0.010$).

Real-time PCR confirmation of RNA expression profiles. Specific primers were designed for five genes, seven pseudogenes, and six noncoding regions that were highly expressed in the tiling array analysis (see Table S1 in the supplemental material). Although *M. leprae* RNA was pretreated with DNase I prior to reverse transcription, the RNA was checked by PCR to exclude possible contamination by genomic DNA (data not shown).

Each primer set generated a specific reverse transcription-PCR product (data not shown). The RNA expression levels determined by real-time PCR analysis were comparable to the signal intensities from the tiling array (Fig. 4). Of interest, coding genes produced higher expression levels in real-time PCR, in contrast to the higher level of pseudogene expression detected by the tiling array.

DISCUSSION

We designed and performed a whole-genome tiling array analysis of *M. leprae* RNA expression and demonstrated that pseudogenes and noncoding regions are not silent but instead are strongly expressed. Statistical analysis indicated that RNA expression from noncoding regions was the highest in both peak (Table 1) and mean (Fig. 3) signal intensities and that RNA expression from genes (ORFs) was the lowest. The reliability of the tiling array results was confirmed in part by a comparison with an ORF array, in which multiple gene-specific

probes were designed (Fig. 1). RNA expression detected by tiling array was also confirmed by quantitative real-time PCR analysis. Therefore, the tiling array was a reliable tool for the detection of specific RNA expression from *M. leprae* genome.

The roles of RNA derived from *M. leprae* noncoding regions and pseudogenes are not known, but the aberrant expression of pseudogenes has been reported in some cancers (22, 35). In addition, a nitric oxide synthase pseudogene is expressed in the central nervous system of the snail *Lymnaea stagnalis*, and its transcript is thought to have antisense activities (18). Pseudogenes also have some biological functions in processes such as cell growth and organogenesis (16). Computational analysis of the mouse genome showed that 10% of the mRNA fraction can be derived from pseudogenes (11). Our results suggest that pseudogenes and genes are similarly transcribed. If some pseudogenes function to regulate gene expression, it may explain why *M. leprae* is able to survive with only a limited number of protein-coding genes. Comprehensive analysis of small RNA revealed that small interfering RNAs are expressed from pseudogenes and regulate gene expression (37). In this study, we found that pseudogenes in the functional categories of "degradation" and "energy metabolism" in the "small-molecule metabolism" class were strongly transcribed on a frequent basis. Further functional analysis is needed to elucidate their roles and the reason behind the biased transcription between functional classes. One hypothesis is that pseudogenes are transcribed because the organism has not yet evolved so as to switch them off. The strength of the selective pressure in *M. leprae* to dispense with useless transcription is unclear.

It has been speculated that the massive genomic degeneration seen in *M. leprae* is the result of dysfunctional sigma factors (23). Up to 2% of the *M. leprae* genome consists of repetitive DNA sequences, potential remnants of past transposons (6). Such repetitive sequences are found in pseudogenes in the "other functions" class and in noncoding regions. Of interest, we detected high RNA expression from those regions, suggesting the existence of functional roles now and/or in the past. *Mycobacterium ulcerans*, a close relative of *M. leprae*, has a similar genome structure. *M. ulcerans* has 771 pseudogenes, but the proportion of pseudogenes based on genome size is about 40% of that of *M. leprae* (34). It was also shown that *Mycobacterium marinum* has 65 pseudogenes (33). These species appear to have preserved past genomic evolution and heterotrophic circumstances as they adapted.

Except for rRNA and tRNA, noncoding RNAs are classified as components of ribonucleoproteins, ribozymes, or microRNA; the rest are thought to be junk derived from transposons or splicing remnants (25). The noncoding region occupying one-quarter of the *M. leprae* genome was presumed to be silent. The highly expressed areas of the noncoding regions were thought to be derived from RLEP and LEPREP (6). However, a large number of other noncoding regions that are more highly expressed than genes and pseudogenes have no homology with known sequences of noncoding RNA. Consequently, these RNAs might have a hitherto unrecognized function.

Different classes of *M. leprae* genes exhibited different levels of RNA expression. RNA expression was relatively high from genes in the "small-molecule metabolism" class related to amino acid and nucleotide synthesis, probably because these

small molecules are necessary for protein and RNA synthesis. Moreover, a low level of pseudogene expression in these classification subsets may support the idea that the genes in this class have very essential roles. Similarly, highly expressed genes in the "cell processes" class are responsible for the folding of synthesized proteins. On the other hand, genes related to DNA replication were not strongly expressed, reflecting the fact that the proliferation of *M. leprae* is very slow. Also, although high expression was not detected in some functional subclasses, such as the "biosynthesis of cofactors, prosthetic groups, and carriers" and "degradation of macromolecules" subclasses, these genes are expressed at a low level (data not shown). In fact, genes targeted by particular drugs are included in these subsets. Thus, RNA polymerase III and folic acid synthesis genes, targeted by rifampin and dapsone, respectively (8), are not highly expressed (data not shown). These data indicate that high RNA expression does not necessarily correlate with the functional importance of the genes, such as those related to drug resistance.

High expression was detected from lipoproteins and the PE and PPE families, which is characteristic of *M. leprae*. Lipoproteins function in infection and survival, as exemplified in *M. tuberculosis* (38). The PE and PPE families are specific to *Mycobacterium* species and by definition contain a Pro-Glu or Pro-Pro-Glu motif near the N terminus (4). Since the PE and PPE families are associated with the early secreted antigenic target 6-kDa (ESAT-6) antigen (29), they may play an important role in virulence. Because *M. leprae* has fewer PE, PPE, and ESAT-6-like genes than *M. tuberculosis*, information on these expressed genes will facilitate further functional analysis of a PE, PPE, and ESAT-6-like protein complex.

There were some differences in the levels of RNA expression detected by tiling array and real-time PCR. The level of expression from coding genes detected by tiling array was lower than the level from these genes detected by real-time PCR, while pseudogene expression was more abundant in the tiling array analysis than in real-time PCR. This discrepancy might reflect the difference in the target length for these methods as well as the difference in the length of transcribed RNA.

The genome size of microbes, as well as the proportion of noncoding regions, is much smaller than that of eukaryotes. Therefore, RNA expression from these regions has been extensively studied. One such study resulted in the discovery of an essential protein homolog, Argonaute, which is necessary for microRNA maturation (13). RNA expression from noncoding regions was also detected from the whole-genome analyses of *E. coli* (39) as well as *Prochlorococcus* and *Synechococcus* spp. (3). The tiling array has facilitated far more in-depth transcriptome analysis, including noncoding regions, than previous techniques such as shotgun cloning (1). For example, a *Saccharomyces cerevisiae* tiling array analysis identified 98 novel noncoding RNAs (32). The present tiling array will be similarly useful for the identification of noncoding RNA in bacteria (31) and for further functional analysis. This is the first genome-wide expression profile of *M. leprae* genes, pseudogenes, and noncoding regions, which can used as the foundation for the screening of drug candidates and the study of host-bacillus interactions.

REFERENCES

1. Altuvia, S. 2007. Identification of bacterial small non-coding RNAs: experimental approaches. Curr. Opin. Microbiol. 10:257–261.
2. Ang, S., C. Z. Lee, K. Peck, M. Sindici, U. Matrubutham, M. A. Gleeson, and J. T. Wang. 2001. Acid-induced gene expression in *Helicobacter pylori*: study in genomic scale by microarray. Infect. Immun. 69:1679–1686.
3. Axmann, I. M., P. Kensche, J. Vogel, S. Kohl, H. Herzel, and W. R. Hess. 2005. Identification of cyanobacterial non-coding RNAs by comparative genome analysis. Genome Biol. 6:R73.
4. Cole, S. T., R. Brosch, J. Parkhill, T. Garnier, C. Churcher, D. Harris, S. V. Gordon, K. Eiglmeier, S. Gas, C. E. Barry III, F. Tekaia, K. Badcock, D. Basham, D. Brown, T. Chillingworth, R. Connor, R. Davies, K. Devlin, T. Feltwell, S. Gentles, N. Hamlin, S. Holroyd, T. Hornsby, K. Jagels, A. Krogh, J. McLean, S. Moule, L. Murphy, K. Oliver, J. Osborne, M. A. Quail, M.-A. Rajandream, J. Rogers, S. Rutter, K. Seeger, J. Skelton, R. Squares, S. Squares, J. E. Sulston, K. Taylor, S. Whitehead, and B. G. Barrell. 1998. Deciphering the biology of *Mycobacterium tuberculosis* from the complete genome sequence. Nature 393:537–544.
5. Cole, S. T., K. Eiglmeier, J. Parkhill, K. D. James, N. R. Thomson, P. R. Wheeler, N. Honoré, T. Garnier, C. Churcher, D. Harris, K. Mungall, D. Basham, D. Brown, T. Chillingworth, R. Connor, R. M. Davies, K. Devlin, S. Duthoy, T. Feltwell, A. Fraser, N. Hamlin, S. Holroyd, T. Hornsby, K. Jagels, C. Lacroix, J. Maclean, S. Moule, L. Murphy, K. Oliver, M. A. Quail, M.-A. Rajandream, K. M. Rutherford, S. Rutter, K. Seeger, S. Simon, M. Simmonds, J. Skelton, R. Squares, S. Squares, K. Stevens, K. Taylor, S. Whitehead, J. R. Woodward, and B. G. Barrell. 2001. Massive gene decay in the leprosy bacillus. Nature 409:1007–1011.
6. Cole, S. T., P. Supply, and N. Honoré. 2001. Repetitive sequences in *Mycobacterium leprae* and their impact on genome plasticity. Lepr. Rev. 72:449–461.
7. D'Errico, I., G. Gadaleta, and C. Saccone. 2004. Pseudogenes in metazoa: origin and features. Brief. Funct. Genomics Proteomics 3:157–167.
8. Dhople, A. M. 2000. Search for newer antileprosy drugs. Indian J. Lepr. 72:5–20.
9. Faucher, S. P., S. Porwollik, C. M. Dozois, M. McClelland, and F. Daigle. 2006. Transcriptome of *Salmonella enterica* serovar Typhi within macrophages revealed through the selective capture of transcribed sequences. Proc. Natl. Acad. Sci. USA 103:1906–1911.
10. Franchini, A. G., and T. Egli. 2006. Global gene expression in *Escherichia coli* K-12 during short-term and long-term adaptation to glucose-limited continuous culture conditions. Microbiology 152:2111–2127.
11. Frith, M. C., L. G. Wilming, A. Forrest, H. Kawaji, S. L. Tan, C. Wahlestedt, V. B. Bajic, C. Kai, J. Kawai, P. Carninci, Y. Hayashizaki, T. L. Bailey, and L. Huminiecki. 2006. Pseudo-messenger RNA: phantoms of the transcriptome. PLoS Genet. 2:e23.
12. Gottesman, S. 2004. The small RNA regulators of *Escherichia coli*: roles and mechanisms. Annu. Rev. Microbiol. 58:303–328.
13. Hall, T. M. 2005. Structure and function of argonaute proteins. Structure 13:1403–1408.
14. Hirotsune, S., N. Yoshida, A. Chen, L. Garrett, F. Sugiyama, S. Takahashi, K. Yagami, A. Wynshaw-Boris, and A. Yoshiki. 2003. An expressed pseudogene regulates the messenger-RNA stability of its homologous coding gene. Nature 423:91–96.
15. Kampa, D., J. Cheng, P. Kapranov, M. Yamanaka, S. Brubaker, S. Cawley, J. Drenkow, A. Piccolboni, S. Bekiranov, G. Helt, H. Tammana, and T. R. Gingeras. 2004. Novel RNAs identified from an in-depth analysis of the transcriptome of human chromosomes 21 and 22. Genome Res. 14:331–342.
16. Kandouz, M., A. Bier, G. D. Carystinos, M. A. Alaoui-Jamali, and G. Batist. 2004. Connexin43 pseudogene is expressed in tumor cells and inhibits growth. Oncogene 23:4763–4770.
17. Kin, T., K. Yamada, G. Terai, H. Okida, Y. Yoshinari, Y. Ono, A. Kojima, Y. Kimura, T. Komori, and K. Asai. 2007. fRNAdb: a platform for mining/annotating functional RNA candidates from non-coding RNA sequences. Nucleic Acids Res. 35:D145–D148.
18. Korneev, S. A., J. H. Park, and M. O'Shea. 1999. Neuronal expression of neural nitric oxide synthase (nNOS) protein is suppressed by an antisense RNA transcribed from an NOS pseudogene. J. Neurosci. 19:7711–7720.

19. Lawrence, J. G., R. W. Hendrix, and S. Casjens. 2001. Where are the pseudogenes in bacterial genomes? Trends Microbiol. 9:535–540.
20. Lin, H., A. Shabbir, M. Molnar, and T. Lee. 2007. Stem cell regulatory function mediated by expression of a novel mouse Oct4 pseudogene. Biochem. Biophys. Res. Commun. 355:111–116.
21. Liu, Y., P. M. Harrison, V. Kunin, and M. Gerstein. 2004. Comprehensive analysis of pseudogenes in prokaryotes: widespread gene decay and failure of putative horizontally transferred genes. Genome Biol. 5:R64.
22. Lu, W., D. Zhou, G. Glusman, A. G. Utleg, J. T. White, P. S. Nelson, T. J. Vasicek, L. Hood, and B. Lin. 2006. KLK31P is a novel androgen regulated and transcribed pseudogene of kallikreins that is expressed at lower levels in prostate cancer cells than in normal prostate cells. Prostate 66:936–944.
23. Madan Babu, M. 2003. Did the loss of sigma factors initiate pseudogene accumulation in *M. leprae*? Trends Microbiol. 11:59–61.
24. Mattick, J. S. 2001. Non-coding RNAs: the architects of eukaryotic complexity. EMBO Rep. 2:986–991.
25. Mattick, J. S., and I. V. Makunin. 2006. Non-coding RNA. Hum. Mol. Genet. 15(special no. 1):R17–R29.
26. Nakata, N., M. Matsuoka, Y. Kashiwabara, N. Okada, and C. Sasakawa. 1997. Nucleotide sequence of the *Mycobacterium leprae katG* region. J. Bacteriol. 179:3053–3057.
27. Niehus, E., H. Gressmann, F. Ye, R. Schlapbach, M. Dehio, C. Dehio, A. Stack, T. F. Meyer, S. Suerbaum, and C. Josenhans. 2004. Genome-wide analysis of transcriptional hierarchy and feedback regulation in the flagellar system of *Helicobacter pylori*. Mol. Microbiol. 52:947–961.
28. Ochman, H., and L. M. Davalos. 2006. The nature and dynamics of bacterial genomes. Science 311:1730–1733.
29. Okkels, L. M., and P. Andersen. 2004. Protein-protein interactions of proteins from the ESAT-6 family of *Mycobacterium tuberculosis*. J. Bacteriol. 186:2487–2491.
30. Overton, T. W., L. Griffiths, M. D. Patel, J. L. Hobman, C. W. Penn, J. A. Cole, and C. Constantinidou. 2006. Microarray analysis of gene regulation by oxygen, nitrate, nitrite, FNR, NarL and NarP during anaerobic growth of *Escherichia coli*: new insights into microbial physiology. Biochem. Soc. Trans. 34:104–107.
31. Rivas, E., R. J. Klein, T. A. Jones, and S. R. Eddy. 2001. Computational identification of noncoding RNAs in *E. coli* by comparative genomics. Curr. Biol. 11:1369–1373.
32. Samanta, M. P., W. Tongprasit, H. Sethi, C. S. Chin, and V. Stolc. 2006. Global identification of noncoding RNAs in *Saccharomyces cerevisiae* by modulating an essential RNA processing pathway. Proc. Natl. Acad. Sci. USA 103:4192–4197.
33. Stinear, T. P., T. Seemann, P. F. Harrison, G. A. Jenkin, J. K. Davies, P. D. Johnson, Z. Abdellah, C. Arrowsmith, T. Chillingworth, C. Churcher, K. Clarke, A. Cronin, P. Davis, I. Goodhead, N. Holroyd, K. Jagels, A. Lord, S. Moule, K. Mungall, H. Norbertczak, M. A. Quail, E. Rabbinowitsch, D. Walker, B. White, S. Whitehead, P. L. Small, R. Brosch, L. Ramakrishnan, M. A. Fischbach, J. Parkhill, and S. T. Cole. 2008. Insights from the complete genome sequence of *Mycobacterium marinum* on the evolution of *Mycobacterium tuberculosis*. Genome Res. 18:729–741.
34. Stinear, T. P., T. Seemann, S. Pidot, W. Frigui, G. Reysset, T. Garnier, G. Meurice, D. Simon, C. Bouchier, L. Ma, M. Tichit, J. L. Porter, J. Ryan, P. D. Johnson, J. K. Davies, G. A. Jenkin, P. L. Small, L. M. Jones, F. Tekaia, F. Laval, M. Daffe, J. Parkhill, and S. T. Cole. 2007. Reductive evolution and niche adaptation inferred from the genome of *Mycobacterium ulcerans*, the causative agent of Buruli ulcer. Genome Res. 17:192–200.
35. Suo, G., J. Han, X. Wang, J. Zhang, Y. Zhao, and J. Dai. 2005. Oct4 pseudogenes are transcribed in cancers. Biochem. Biophys. Res. Commun. 337:1047–1051.
36. Suzuki, K., N. Nakata, P. D. Bang, N. Ishii, and M. Makino. 2006. High-level expression of pseudogenes in *Mycobacterium leprae*. FEMS Microbiol. Lett. 259:208–214.
37. Tanigawa, K., K. Suzuki, K. Nakamura, T. Akama, A. Kawashima, H. Wu, M. Hayashi, S. Takahashi, S. Ikuyama, T. Ito, and N. Ishii. 2008. Expression of adipose differentiation-related protein (ADRP) and perilipin in macrophages infected with *Mycobacterium leprae*. FEMS Microbiol. Lett. 289:72–79.
38. Vandal, O. H., L. M. Pierini, D. Schnappinger, C. F. Nathan, and S. Ehrt. 2008. A membrane protein preserves intrabacterial pH in intraphagosomal *Mycobacterium tuberculosis*. Nat. Med. 14:849–854.
39. Vogel, J., V. Bartels, T. H. Tang, G. Churakov, J. G. Slagter-Jager, A. Huttenhofer, and E. G. Wagner. 2003. RNomics in *Escherichia coli* detects new sRNA species and indicates parallel transcriptional output in bacteria. Nucleic Acids Res. 31:6435–6443.
40. Yogi, Y., T. Banba, M. Kobayashi, H. Katoh, N. Jahan, M. Endoh, and H. Nomaguchi. 1999. Leprosy in hypertensive nude rats (SHR/NCrj-*rnu*). Int. J. Lepr. Other Mycobact. Dis. 67:435–445.
41. Yogi, Y., M. Endoh, T. Banba, M. Kobayashi, H. Katoh, K. Suzuki, and H. Nomaguchi. 2002. Susceptibility to *Mycobacterium leprae* of congenic hypertensive nude rat (SHR/NCrj-*rnu*) and production of cytokine from the resident peritoneal macrophages. Jpn. J. Lepr. 71:39–45. (In Japanese.)
42. Zhou, D., Y. Han, J. Qiu, L. Qin, Z. Guo, X. Wang, Y. Song, Y. Tan, Z. Du, and R. Yang. 2006. Genome-wide transcriptional response of *Yersinia pestis* to stressful conditions simulating phagolysosomal environments. Microbes Infect. 8:2669–2678.

Tryptophan aspartate-containing coat protein (CORO1A) suppresses Toll-like receptor signalling in *Mycobacterium leprae* infection

K. Tanigawa,* K. Suzuki,* H. Kimura,†
F. Takeshita,‡ H. Wu,* T. Akama,*
A. Kawashima* and N. Ishii*

*Department of Bioregulation, Leprosy Research
Center, National Institute of Infectious Diseases,
Higashimurayama, Tokyo, Japan, †Department of
Pathology, The Johns Hopkins School of Medicine,
Baltimore, MD, USA, and ‡Department of
Molecular Biodefense Research, Yokohama City
University School of Medicine, Kanazawa-ku,
Yokohama, Japan

Summary

Mycobacterium leprae is an intracellular pathogen that survives within the phagosome of host macrophages. Several host factors are involved in producing tolerance, while others are responsible for killing the mycobacterium. Tryptophan aspartate-containing coat protein (TACO; also known as CORO1A or coronin-1) inhibits the phagosome maturation that allows intracellular parasitization. In addition, the Toll-like receptor (TLR) activates the innate immune response. Both CORO1A and TLR-2 co-localize on the phagosomal membrane in the dermal lesions of patients with lepromatous leprosy. Therefore, we hypothesized that CORO1A and TLR-2 might interact functionally. This hypothesis was tested by investigating the effect of CORO1A in TLR-2-mediated signalling and, inversely, the effect of TLR-2-mediated signalling on CORO1A expression. We found that CORO1A suppresses TLR-mediated signal activation in human macrophages, and that TLR2-mediated activation of the innate immune response resulted in suppression of CORO1A expression. However, *M. leprae* infection inhibited the TLR-2-mediated CORO1A suppression and nuclear factor-κB activation. These results suggest that the balance between TLR-2-mediated signalling and CORO1A expression will be key in determining the fate of *M. leprae* following infection.

Keywords: CORO1A, leprosy, *Mycobacterium leprae*, phagosome, TLR

Introduction

Pathogen recognition systems, which include the Toll-like receptors (TLRs), melanoma differentiation-associated gene 5 and retinoic acid-inducible gene-1, function as biosensors for infection. Upon infection, activation of the innate immune system not only induces a primary biodefensive reaction, but is essential for activation of the adaptive immune system. TLRs are the pattern recognition receptors that sense and distinguish pathogen-associated molecular patterns that are found on a broad range of infectious agents [1]. TLRs also play an essential role in the eradication of engulfed pathogens [2,3]. Of the 13 known TLRs, TLR-2, in combination with TLR-1 or TLR-6, is responsible for the recognition of mycobacteria [4,5]. Bacterial and fungal cell wall components, such as peptidoglycan (PGN), lipoarabinomannan (LAM) and zymosan are well-known ligands of TLR-2 [6]. Notably, several studies have demonstrated that TLR-2 is recruited and localized to the phagosomal membrane following exposure to its ligands [7,8]

Macrophages play a central role in the innate immune system. They use cell surface TLR-2 and TLR-4 to recognize PGN, LAM or lipopolysaccharide (LPS), which stimulates phagocytosis and destruction of bacterial pathogens. Therefore, macrophages are part of the principal host defence system that operates during the early period of infection. However, some intracellular microorganisms evade detection and survive. It is thought that they reside and proliferate within cells by changing the intracellular environment. However, there is no one escape mechanism, and many have evolved their own strategies for intracellular survival. *Mycobacterium bovis* bacille Calmette-Guérin (*M. bovis* BCG) utilizes a host protein, tryptophan aspartate-containing coat protein (TACO; also known as CORO1A or coronin-1), to escape detection by the immune system [9]. Upon *M. bovis* BCG infection, CORO1A is recruited, in association with tubulin, from the plasma membrane to the phagosomal membrane to play an essential role in inhibiting the phagosome–lysosome fusion, as well as in the survival of bacilli within macrophages. The phagosomal localization is transient in macrophages exposed to dead mycobacteria,

whereas localization is quite stable when live bacilli are used. *M. bovis* BCG was digested completely in liver Küpffer cells, which lack CORO1A expression [9]. In addition, *M. tuberculosis* uses CORO1A to activate Ca^{2+}-dependent phosphatase calcineurin, which blocks phagosome–lysosome fusion [10,11].

The *M. leprae*, the aetiological agent of leprosy, is a highly successful intracellular pathogen. *M. leprae* can survive within macrophage phagosomes as well as *M. bovis* and *M. tuberculosis*. We have reported recently that both TLR-2 and CORO1A localize on the membrane of phagosomes containing *M. leprae* [12]. However, the association between TLR-2 and CORO1A in leprosy is unknown. The goal of the present study was to investigate the functional interaction between two host proteins, CORO1A and TLR-2, which have opposing effects on the intracellular survival of *M. leprae*.

Materials and methods

Cell culture and infection

The human promonocytic cell line THP-1 was obtained from the American Type Culture Collection (ATCC; Manassas, VA, USA). They were cultured in 10-cm tissue culture dishes in RPMI-1640 medium supplemented with 10% charcoal-treated fetal bovine serum (FBS), 2% non-essential amino acids and 50 mg/ml penicillin/streptomycin at 37°C in 5% CO_2. Human embryonic kidney 293 (HEK293) cells were obtained from ATCC. Cells were maintained in Dulbecco's modified Eagle's medium, supplemented with 10% heat-inactivated FBS and 50 mg/ml of penicillin/streptomycin at 37°C in 5% CO_2. *M. leprae* was prepared from the footpads of nude mice as described [12]. In some experiments, THP-1 cells were differentiated into macrophages by incubation in 50 nM phorbol myristate acetate (PMA) for 24 h before use.

Plasmid preparation

The cDNA encoding human CORO1A was polymerase chain reaction (PCR)-amplified using cDNA prepared from THP-1 cells and introduced into the *MluI-XbaI* site of the pCIneo mammalian expression vector (Promega, Madison, WI, USA). The cDNAs encoding human TLR-2 and TLR-3 were purchased from InvivoGen (San Diego, CA, USA) and transferred to the pGA mammalian expression vector [13]. Human TLR expression plasmids were made using a luciferase reporter plasmid, p5×nuclear factor (NF)-κB-luc, purchased from Stratagene (La Jolla, CA, USA). pGL3 h interferon (IFN)-β was constructed using the human IFN-β promoter region −110 to +20 (relative to the transcription initiation site), which was PCR-amplified from human genomic DNA and cloned into the pGL3 basic luciferase reporter plasmid (Promega). The pGL3 control vector, with a cytomegalovirus (CMV) promoter, was also purchased

from Promega. The sequences of the PCR products were verified using an ABI PRISM Genetic Analyzer (Applied Biosystems, Foster City, CA, USA).

Transfection and reporter gene assay

The HEK293 (2×10^4) or THP-1 (1×10^6) cells were used in the reporter gene assays. Transfection into THP-1 cells was conducted using diethylaminoethyl-dextran [14]. The HEK293 cells were transfected using FuGene 6 (Roche Applied Science, Indianapolis, IN, USA) according to the manufacturer's protocol [15]. HEK293 cells were transfected with 40 ng of a human TLR expression plasmid (TLR-2, TLR-3 or TLR-4) in the presence or absence of 40, 80, 160 or 320 ng of CORO1A expression plasmid and 25 ng of either luciferase reporter plasmid (p5×NF-κB-luc), pGL3 Control or pGL3-hIFNβ. The total amount of DNA was adjusted using empty CMV4 plasmid. Cells were incubated for 36 h after transfection and then treated with 2 μg/ml PGN from *Staphylococcus aureus* (Sigma, St Louis, MO, USA) or *M. leprae*, poly(IC) (50 μg/ml), LPS (1 μg/ml) or tumour necrosis factor (TNF)-α (50 μg/ml) for an additional 12 h. Luciferase activity was measured using the luciferase reporter assay system (Promega) according to the manufacturer's protocol [15,16]. To simulate infection, cells were incubated for 36 h after transfection of p5×NF-κB-luc, then treated with 2 μg/ml PGN and either live or heat-killed *M. leprae* (multiplicity of infection: 10), or a combination of the two for 12 h. Latex beads were used as a negative control for *M. leprae* infection.

Western blot analysis

Cells were lysed in a buffer containing 50 mM HEPES, 150 mM NaCl, 5 mM ethylenediamine tetraacetic acid, 0·1% NP40, 20% glycerol and protease inhibitor cocktail (Complete Mini; Roche) for 1 h. Samples were heated in sodium dodecyl sulphate (SDS) sample loading buffer (Invitrogen, Carlsbad, CA, USA) at 80°C for 10 min, then loaded onto a 10% denaturing SDS-Tris-glycine gel (Invitrogen). After electrophoresis, proteins were transferred to a polyvinylidene membrane (Invitrogen). The membrane was washed with phosphate-buffered saline 0·1% Tween 20 (PBST), blocked with PBST containing 5% non-fat milk, and incubated with TACO antibodies. The membrane was probed subsequently with biotinylated donkey anti-rabbit antibodies and streptavidin–horseradish peroxidase (GE Healthcare, Buckinghamshire, UK) according to the manufacturer's protocol, and then developed using the ECL Plus Western Blotting Detection Reagents (GE Healthcare).

Reverse transcription PCR and real-time PCR

RNA was prepared using RNeasy Mini Kits (Qiagen Inc., Valencia, CA, USA) with minor modifications of the manu-

facturer's protocol, as described previously [16,17]. Briefly, cells were washed with Dulbecco's phosphate-buffered saline, resuspended in 600 μl of lysis solution and passed through a QIAshredder. After 600 μl of 70% ethanol was added, the mixture was purified through a spin column, washed with 600 μl of RW1 wash solution, and washed twice with 500 μl of RPE wash solution. Total RNA was eluted with 30 μl of RNase-free water.

To perform the semi-quantitative reverse transcriptional assay, 1 μg of total RNA was reverse-transcribed into cDNA using the high-capacity cDNA reverse transcription kit (Applied Biosystems). Touchdown PCR was adopted to adjust β-actin levels as the endogenous reference housekeeping gene. The following PCR primers were used: human β-actin, 5'-AGCCATGTACGTAGCCATCC-3' (forward) and 5'-TGTGGTGGTGAAGCTGTAGC-3' (reverse); and human CORO1A, 5'-ACCTCCTGCCGTGACAAGCG-3' (forward) 5'-TCCTGGAACAGGTCCGACTTTC-3'(reverse). PCR products were run on a 2% agarose gel.

Relative quantification of CORO1A mRNA expression was also performed with real-time PCR using TaqMan-N-(3-Fluoranthyl) maleimide (FAM)-minor groove binder (MGB) assays and automated analysis in an Applied Biosystems 7000 real-time PCR system (Applied Biosystems). The sequences of the human CORO1A primers were 5'-GTGCGCATCATCGAGCC-3' (forward) and 5'-ACGAACA CTGCACGCACG-3' (reverse). The sequence of the TaqMan probe was 5'FAM-CACTGTCGTAGCTGAGAA-MGB3'. TaqMan β-actin detection reagents (Applied Biosystems) were used as a control.

Statistical analysis

All experiments were repeated at least three times. Statistical significance was evaluated using Student's t-test with $P < 0.05$ considered statistically significant.

Results

CORO1A suppresses TLR-mediated signalling

Although both CORO1A and TLR-2 are expressed in macrophages and play important roles in mycobacterial infection, it is unclear if an interaction exists between the two. CORO1A and TLR-2 are recruited to, and co-localize on, the phagosomal membrane upon *M. leprae* infection [12], even though the two molecules have opposing effects. While CORO1A is involved in the survival of mycobacteria, TLR participates in the elimination of bacterial pathogens by activating the immune system. Thus, the co-localization of both proteins on the membrane of phagosomes that contain *M. leprae* prompted us to determine if there is a functional interaction between CORO1A and TLR.

The effect of CORO1A on the activation of TLR-2-mediated signalling was examined using the THP-1 cell line.
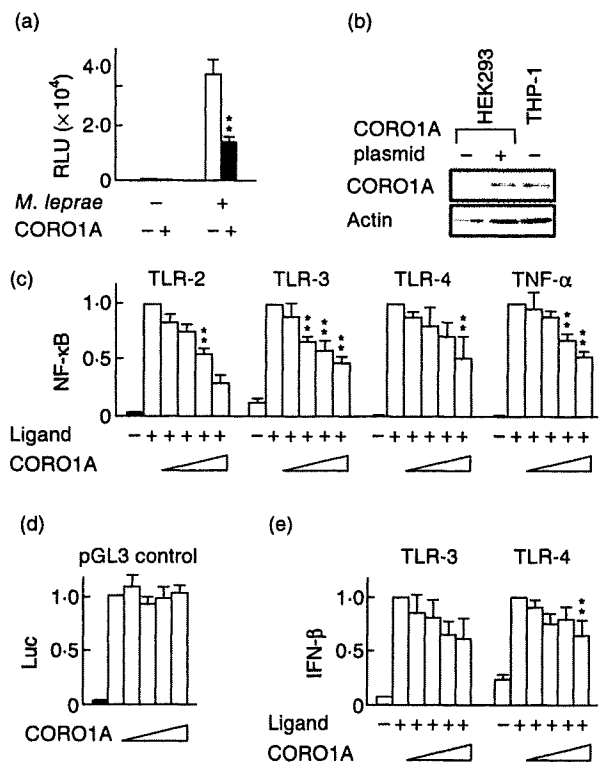

Fig. 1. Tryptophan aspartate-containing coat protein (TACO; also known as CORO1A or coronin-1) suppresses Toll-like receptor (TLR) signalling. The human promonocytic cell line (THP-1) cells were transfected with a luciferase reporter plasmid, p5×nuclear factor (NF)-κB-luc, and incubated for 48 h before the addition of *Mycobacterium leprae* (multiplicity of infection: 10) or peptidoglycan (PGN) (2 μg/ml). Luciferase activity was measured 12 h after stimulation (a). Western blot analysis of CORO1A protein levels in human embryonic kidney 293 (HEK293) cells transfected with a CORO1A expression plasmid and in THP-1 cells (control) demonstrated that the same amount of cellular protein was present in both cell types (b). HEK293 cells were transfected with a luciferase reporter plasmid, p5×NF-κB-luc (c), pGL3-control (d) or pGL3-h interferon (IFN)-β (e) along with the indicated human TLR expression plasmid (TLR-2, TLR-3 or TLR-4) in the presence or absence of the CORO1A expression plasmid. PGN, poly(IC) and lipopolysaccharide (LPS) were used as specific TLR-2, TLR-3 and TLR-4 ligands. Each ligand or tumour necrosis factor (TNF)-α was added 36 h after transfection, and luciferase activity was measured 12 h after ligand stimulation. The results are presented as relative promoter activity in which luciferase activity in the absence of the CORO1A expression plasmid was set to 1·0 (c,d,e). The graph shows the mean ± standard deviation. One asterisk (*) indicates a value of $P < 0.05$, two asterisks (**) indicate a value of $P < 0.01$.

THP-1 cells express functional TLR-2 that can detect PGN and the cell wall glycolipids of *M. leprae* [18]. THP-1 cells transfected with either CORO1A expression plasmid or control plasmid were infected with *M. leprae*. NF-κB activation was evaluated by the measurement of luciferase levels. As shown in Fig. 1a, CORO1A suppressed NF-κB activation

497

induced by *M. leprae* infection. CORO1A also suppressed NF-κB activation induced by PGN stimulation (data not shown).

The specificity of the suppressive effect of CORO1A on NF-κB was investigated using HEK293 cells, which do not express TLR-2. Prior to the experiment, we confirmed that transfection of the CORO1A expression plasmid in HEK293 cells results in an amount of protein comparable to that produced in the THP-1 controls (Fig. 1b). HEK293 cells were co-transfected with hTLR-2 expression plasmid and an NF-κB-dependent luciferase reporter plasmid. Thirty-six hours after transfection, the cells were stimulated with PGN for 12 h and reporter gene activity was analysed. Consistent with the data obtained from THP-1 macrophage cells (Fig. 1a), CORO1A suppressed PGN-induced, TLR-2-mediated NF-κB activity in a dose-dependent manner in HEK293 cells (Fig. 1c). Interestingly, CORO1A suppressed both dsRNA-induced NF-κB activation through TLR-3 and LPS-induced NF-κB activation through TLR-4 in a dose-dependent manner (Fig. 1c). Because TNF-α is a classic cytokine that induces NF-κB activation, it was possible that CORO1A influences the action of TNF-α. Indeed, CORO1A suppressed TNF-α-induced NF-κB activation in a dose-dependent manner (Fig. 1c). Transfection of a plasmid carrying unrelated cDNA had no effect (data not shown). Therefore, suppression was specific to expressed CORO1A. The suppression was also specific to an NF-κB-dependent promoter, because pGL3 control (in which luciferase activity is controlled by the CMV promoter) was not influenced by CORO1A (Fig. 1d). These results suggest that CORO1A suppresses NF-κB activation, most probably by influencing the common signalling pathway shared by TLR and TNF-α. In a similar experiment using an IFN-β promoter-dependent luciferase reporter plasmid, CORO1A suppressed both TLR-3- and TLR-4-mediated IFN-β promoter activity in a dose-dependent manner (Fig. 1e), suggesting that CORO1A helps intracellular pathogens survive by suppressing activation of the innate immune system.

Activation of innate immunity modulates CORO1A expression

The effect of TLR-2-mediated signalling on CORO1A expression was assessed in THP-1 cells. THP-1 cells preactivated by PMA were used to test for an effect of PGN on differentiated macrophages; PGN decreased significantly CORO1A mRNA expression in 6–12 h (Fig. 2a). Quantitative evaluation of CORO1A mRNA levels by real-time PCR confirmed that RNA expression decreased 1/60 in 12 h, but returned to original levels in 24 h (Fig. 2b). CORO1A protein levels decreased 24–48 h after PGN stimulation (Fig. 2c). A similar decrease in CORO1A was induced by 1,25-dihydroxycholecalciferol (Fig. 2d), an active metabolite of 25-hydroxycholecalciferol (vitamin D₃), which activates anti-mycobacterial mechanisms more effectively than IFN-γ
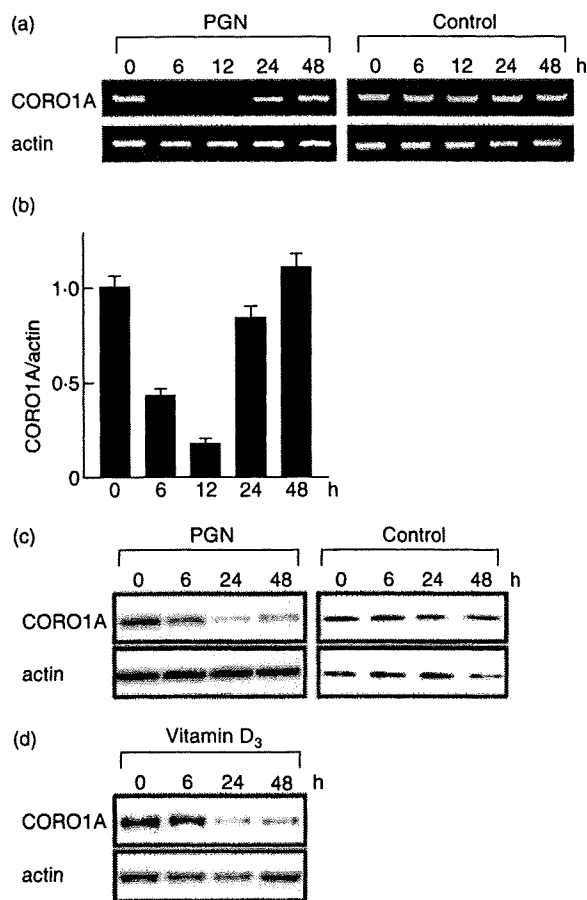

Fig. 2. *Mycobacterium leprae* infection modulates tryptophan aspartate-containing coat protein (TACO; also known as CORO1A or coronin-1) expression. Human promonocytic cell line (THP-1) cells (1 × 10⁶) were cultured in a six-well plate, treated with 20 ng/ml of phorbol myristate acetate (PMA) for 48 h, and incubated with or without 2 µg/ml of peptidoglycan (PGN) (a, b and c) or 1 µM of the active form of vitamin D₃ (1,25-dihydroxycholecalcifenol) (d). After incubating for the indicated time, total RNA and total cellular protein were isolated, and reverse transcription–polymerase chain reaction (a), quantitative real-time PCR (b) and Western blot analysis (c,d) were performed as described in the Materials and methods.

in human macrophages [19]. These data suggest that macrophage activation results in CORO1A suppression regardless of the pathway of activation. Such a decrease in CORO1A protein levels might promote lysosomal fusion, thereby enhancing bacterial elimination within the phagosome.

The *M. leprae* infection modulates CORO1A expression

Although PGN suppressed CORO1A expression significantly (Fig. 2), the addition of *M. leprae* inhibited the ability of PGN to suppress CORO1A mRNA (Fig. 3a) and protein (Fig. 3b) levels, despite the fact that both PGN and *M. leprae*
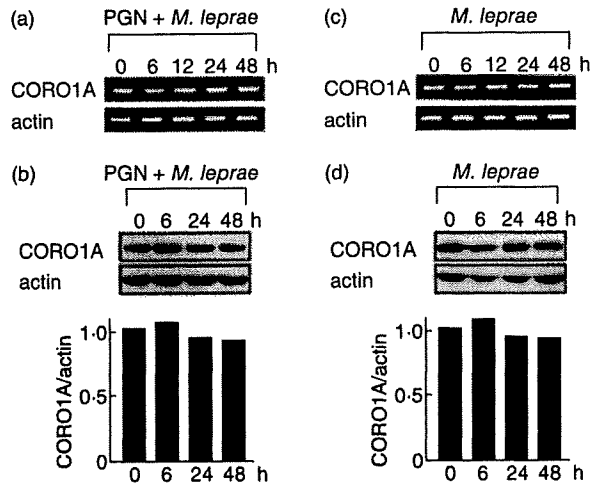
498

Discussion

This study revealed evidence of a functionally inverse relationship between CORO1A and TLRs. In *M. bovis* BCG, CORO1A contributes to survival of bacilli by inhibiting fusion of the lysosome to the phagosome, a suppression that

(a)

(b)

Fig. 3. *Mycobacterium leprae* infection reverses peptidoglycan (PGN)-induced reduction of tryptophan aspartate-containing coat protein (TACO; also known as CORO1A or coronin-1) protein levels. Human promonocytic cell line (THP-1) cells (1×10^6) were cultured in a six-well plate, treated with 20 ng/ml of phorbol myristate acetate (PMA) for 48 h, and stimulated with 2 µg/ml of PGN and/or *M. leprae* (multiplicity of infection: 10). After incubating for the indicated time, total RNA and total cellular protein were purified and reverse transcription–polymerase chain reaction analysis (a,c) and Western blot analysis (b,d) were performed. Densitometric analysis of the specific bands detected in the Western blot is shown in a bar graph.

are recognized by TLR-2 and are capable of activating NF-κB. *M. leprae* infection alone did not modulate CORO1A expression significantly (Fig. 3c and d).

Viable *M. leprae* suppresses TLR-2-mediated NF-κB activation

The modulation of CORO1A after *M. leprae* infection led to the hypothesis that *M. leprae* partially influences TLR-mediated signalling for survival within macrophages by sustaining CORO1A expression levels. To test this hypothesis, THP-1 cells were differentiated into macrophages by PMA, transfected with the NF-κB-dependent luciferase reporter plasmid and stimulated with PGN combined with viable *M. leprae*, heat-killed *M. leprae* or latex beads (control). Although viable and dead *M. leprae* activated NF-κB weakly, only the live bacteria suppressed PGN-induced NF-κB activation, while dead *M. leprae* and the latex beads did not (Fig. 4a). The CORO1A protein levels were suppressed only by PGN treatment, but were maintained by *M. leprae* (Fig. 4b), which corresponds to the results shown in Figs 2 and 3 respectively. PGN-induced suppression of CORO1A protein was counteracted by *M. leprae* (Fig. 4b). These results suggest that *M. leprae* infection antagonizes the suppressive effect of PGN on CORO1A levels, and that live bacilli have the ability to inhibit TLR-2-mediated activation of NF-κB.
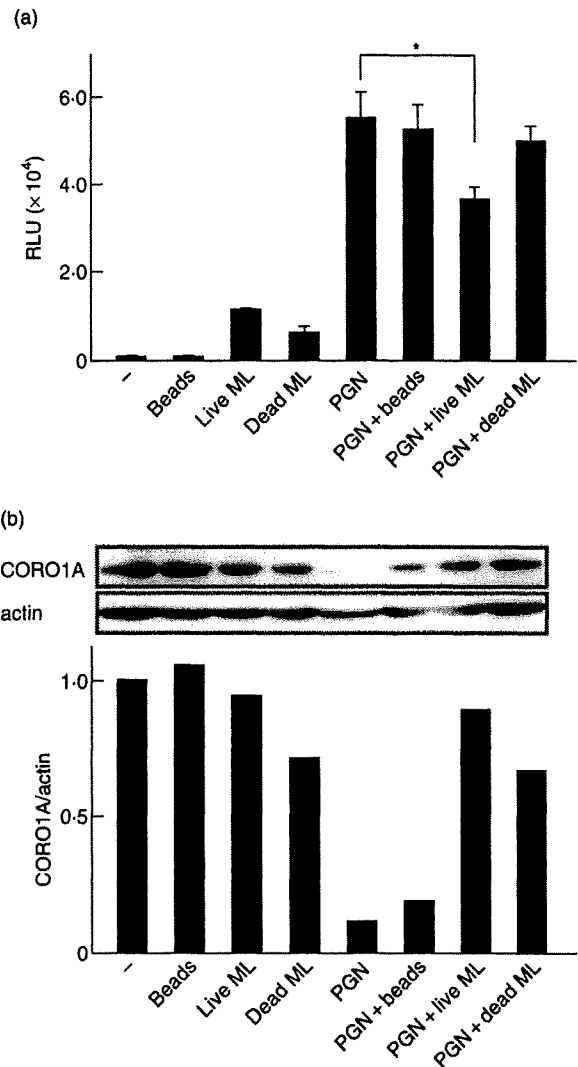
Fig. 4. Viable *Mycobacterium leprae* suppresses Toll-like receptor-2 (TLR-2)-mediated nuclear factor (NF)-κB activation. Human promonocytic cell line (THP-1) cells were transfected with the p5×NF-κB-luc plasmid and stimulated with latex beads, peptidoglycan (PGN) and either viable *M. leprae*, heat-killed (multiplicity of infection: 10) or a combination of the two. The graph shows the mean ± standard deviation of luciferase activity representing NF-κB-dependent promoter activation. The asterisk (*) indicates a value of $P < 0.05$. Three independent experiments produced similar results (a). Total cellular protein was purified 12 h after each treatment and Western blot analysis was performed (b). Densitometric analysis of the specific bands detected in the Western blot is shown in a bar graph.

is abolished when CORO1A is absent [9]. TLR-2, upon recognition of mycobacteria, activates the innate immune response in order to protect cells from infection. The observation that both CORO1A and TLR-2 localize to phagosomal membranes that contain mycobacteria [12] was of interest because of the opposing functions of these two host factors. Previous studies in *M. tuberculosis* or *M. bovis* BCG focused upon the roles of either CORO1A or the TLRs in the process of mycobacterial infection, not their combinatorial effect. We used *M. leprae*, probably the most typical example of an intracellular pathogen, to investigate a possible interaction between CORO1A and TLR. Their co-localization on the phagosomal membrane led us to hypothesize that these two factors might interact, thereby influencing the fate of mycobacteria within infected macrophages.

An interaction between CORO1A and TLR-2 was confirmed using a number of different approaches. Although a physical interaction between CORO1A and TLRs was not observed in immunoprecipitation and yeast two-hybrid assays (data not shown), we found reciprocal antagonism in a functional interaction. CORO1A suppressed TLR-2-mediated NF-κB activation; TLR-3-, TLR-4- and TNF-α-stimulated NF-κB activation; and IFN-β promoter activation. One possible explanation is that CORO1A associates directly with a molecule that is downstream of both TLR and TNF-α signalling, such as NIK (NF-κB inducing kinase), inhibitor (I)κB or NF-κB. Another possibility is that CORO1A associates with other molecules such as nicotinamide adenine dinucleotide phosphate (NADPH) oxidase to suppress TLR signalling indirectly, as components of NADPH oxidase suppress TLR-2-mediated signalling [20]. Regardless of the molecular mechanism, our data suggest clearly that CORO1A not only blocks phagosome–lysosome fusion, but also reduces signalling in the pathways that lead to activation of innate immunity.

Conversely, the activation of macrophage, either by TLRs or the active form of vitamin D_3, resulted in the suppression of CORO1A expression. Although the relationship between TLR and CORO1A is poorly understood, evidence suggests that vitamin D might be a factor that connects these two molecules. Thus, TLR might trigger the vitamin D-mediated human anti-microbial response through induction of cathelicidin [21,22]. Liu *et al.* found that the vitamin D receptor is up-regulated in monocytes stimulated with a synthetic 19-kDa *M. tuberculosis*-derived lipopeptide, and that cathelicidine mediates anti-microbial activity against *M. tuberculosis*. The suppressive effect of vitamin D on CORO1A gene expression was also found in human macrophages [23]. Therefore, it is plausible that activated TLR signalling by mycobacteria suppresses CORO1A expression through vitamin D.

Although PGN suppressed CORO1A expression, *M. leprae* did not affect CORO1A expression significantly despite the fact that *M. leprae* alone can activate NF-κB weakly. Rather, viable *M. leprae* has the ability to suppress TLR-2-mediated

NF-κB activation. The results indicate that *M. leprae* activates NF-κB weakly through TLR-2; however, it suppresses PGN-induced NF-κB activation simultaneously. It has been reported that only viable *M. bovis* BCG can sustain CORO1A on the phagosomal membrane [9]. Therefore, we compared the effect of live and heat-killed *M. leprae* on CORO1A expression. Although there was no significant difference in total CORO1A protein levels between cells treated with viable or dead *M. leprae*, the phagosomal localization of CORO1A, which may affect TLR-2-mediated signalling directly, would differ [9,12]. Innate immune reactions would be activated upon recognition of *M. leprae* at the beginning of infection by TLRs. However, our results suggest that viable *M. leprae* utilizes a hitherto unknown strategy that leads to suppression of innate immune activities, at least in part, through inhibition of NF-κB activation. Although the suppression of PGN-induced NF-κB activation by *M. leprae* detected in this study was significant, the level of reduction was not very striking. However, the *in vivo* biological impact could be much stronger when the long-term parasitization of numerous bacilli within a macrophage is considered. We propose that such a function would be established during the process of successful intracellular parasitization. As a result, *M. leprae* infection maintains CORO1A expression levels and suppresses NF-κB activation.

A similar situation can be found in the regulation of adipophilin/adipose differentiation-related protein (ADRP) expression in *M. leprae*-infected macrophages [24]. Although PGN suppresses ADRP expression, infection by *M. leprae* inhibits the suppression. Therefore, it was speculated that live *M. leprae* actively induces and supports ADRP expression to facilitate the accumulation of lipids within the phagosome and to maintain a suitable environment for intracellular survival within macrophages [24]. Unlike other mycobacteria, *M. leprae* is not capable of activating dendritic cell-mediated T cell responses [25,26]. Our results may explain these previous observations by providing evidence that *M. leprae* suppresses NF-κB activation.

As reported previously, *M. leprae* can stimulate TLR-2, even though the stimulation is not as strong as that produced by purified PGN in *in vitro* experiments. The bacterial component that stimulates TLR-2 and activates NF-κB will be PGN or LAM on the *M. leprae* cell wall. In this study, we found that infection with viable *M. leprae* attenuates PGN-induced NF-κB activation, although the molecular mechanisms responsible have yet to be identified. This study demonstrates that *M. leprae* uses a host protein, CORO1A, to inhibit TLR-mediated signalling in order to create an environment more suited for survival. When macrophages are infected by mycobacteria, both killing and tolerant mechanisms are activated. A balance between activation and suppression of NF-κB by *M. leprae* might modulate disease severity after infection and affect the fate of infected bacilli, i.e. successful rejection or parasitization. Understanding their escape mechanisms will provide new ideas for the

development of pharmaceutical or therapeutic strategies to fight pathogens.

References

1 Akira S, Takeda K. Toll-like receptor signalling. Nat Rev Immunol 2004; 4:499–511.

2 Blander JM, Medzhitov R. Regulation of phagosome maturation by signals from Toll-like receptors. Science 2004; 304:1014–18.

3 Brattig NW, Bazzocchi C, Kirschning CJ et al. The major surface protein of Wolbachia endosymbionts in filarial nematodes elicits immune responses through TLR2 and TLR4. J Immunol 2004; 173:437–45.

4 Ozinsky A, Smith KD, Hume D, Underhill DM. Co-operative induction of pro-inflammatory signaling by Toll-like receptors. J Endotoxin Res 2000; 6:393–6.

5 Underhill DM, Ozinsky A, Smith KD, Aderem A. Toll-like receptor-2 mediates mycobacteria-induced proinflammatory signaling in macrophages. Proc Natl Acad Sci USA 1999; 96:14459–63.

6 Takeuchi O, Hoshino K, Akira S. Cutting edge: TLR2-deficient and MyD88-deficient mice are highly susceptible to Staphylococcus aureus infection. J Immunol 2000; 165:5392–6.

7 Underhill DM, Ozinsky A, Hajjar AM et al. The Toll-like receptor 2 is recruited to macrophage phagosomes and discriminates between pathogens. Nature 1999; 401:811–15.

8 Ozinsky A, Underhill DM, Fontenot JD et al. The repertoire for pattern recognition of pathogens by the innate immune system is defined by cooperation between toll-like receptors. Proc Natl Acad Sci USA 2000; 97:13766–71.

9 Ferrari G, Langen H, Naito M, Pieters J. A coat protein on phagosomes involved in the intracellular survival of mycobacteria. Cell 1999; 97:435–47.

10 Jayachandran R, Sundaramurthy V, Combaluzier B et al. Survival of mycobacteria in macrophages is mediated by coronin 1-dependent activation of calcineurin. Cell 2007; 130:37–50.

11 Trimble WS, Grinstein S. TB or not TB: calcium regulation in mycobacterial survival. Cell 2007; 130:12–14.

12 Suzuki K, Takeshita F, Nakata N, Ishii N, Makino M. Localization of CORO1A in the macrophages containing Mycobacterium leprae. Acta Histochem Cytochem 2006; 39:107–12.

13 Ross TM, Xu Y, Bright RA, Robinson HL. C3d enhancement of antibodies to hemagglutinin accelerates protection against influenza virus challenge. Nat Immunol 2000; 1:127–31.

14 Suzuki K, Lavaroni S, Mori A et al. Autoregulation of thyroid-specific gene transcription by thyroglobulin. Proc Natl Acad Sci USA 1998; 95:8251–6.

15 Takeshita F, Suzuki K, Sasaki S, Ishii N, Klinman DM, Ishii KJ. Transcriptional regulation of the human TLR9 gene. J Immunol 2004; 173:2552–61.

16 Suzuki K, Mori A, Saito J, Moriyama E, Ullianich L, Kohn LD. Follicular thyroglobulin suppresses iodide uptake by suppressing expression of the sodium/iodide symporter gene. Endocrinology 1999; 140:5422–30.

17 Suzuki K, Kobayashi Y, Katoh R, Kohn LD, Kawaoi A. Identification of thyroid transcription factor-1 in C cells and parathyroid cells. Endocrinology 1998; 139:3014–17.

18 Krutzik SR, Ochoa MT, Sieling PA et al. Activation and regulation of Toll-like receptors 2 and 1 in human leprosy. Nat Med 2003; 9:525–32.

19 Wang TT, Nestel FP, Bourdeau V et al. Cutting edge: 1,25-dihydroxyvitamin D3 is a direct inducer of antimicrobial peptide gene expression. J Immunol 2004; 173:2909–12.

20 Takeshita F, Ishii KJ, Kobiyama K et al. TRAF4 acts as a silencer in TLR-mediated signaling through the association with TRAF6 and TRIF. Eur J Immunol 2005; 35:2477–85.

21 Liu PT, Stenger S, Li H et al. Toll-like receptor triggering of a vitamin D-mediated human antimicrobial response. Science 2006; 311:1770–3.

22 Liu PT, Stenger S, Tang DH, Modlin RL. Cutting edge: vitamin D-mediated human antimicrobial activity against Mycobacterium tuberculosis is dependent on the induction of cathelicidin. J Immunol 2007; 179:2060–3.

23 Anand PK, Kaul D. Vitamin D3-dependent pathway regulates TACO gene transcription. Biochem Biophys Res Commun 2003; 310:876–7.

24 Tanigawa K, Suzuki K, Nakamura K et al. Expression of adipose differentiation-related protein (ADRP) and perilipin in macrophages infected with Mycobacterium leprae. FEMS Microbiol Lett 2008; 289:72–9.

25 Hashimoto K, Maeda Y, Kimura H et al. Mycobacterium leprae infection in monocyte-derived dendritic cells and its influence on antigen-presenting function. Infect Immun 2002; 70:5167–76.

26 Murray RA, Siddiqui MR, Mendillo M, Krahenbuhl J, Kaplan G. Mycobacterium leprae inhibits dendritic cell activation and maturation. J Immunol 2007; 178:338–44.

Short communication

Detection of RNA expression from pseudogenes and non-coding genomic regions of *Mycobacterium leprae*

Kazuaki Nakamura, Takeshi Akama, Pham Dang Bang, Shin Sekimura, Kazunari Tanigawa, Huhehasi Wu, Akira Kawashima, Moyuru Hayashi, Koichi Suzuki*, Norihisa Ishii

Department of Bioregulation, Leprosy Research Center, National Institute of Infectious Diseases, 4-2-1 Aoba-cho, Higashimurayama, Tokyo 189-0002, Japan

ARTICLE INFO

ABSTRACT

We have previously reported that some pseudogenes are expressed in *Mycobacterium leprae* (*M. leprae*), the causative agent of leprosy, and that their expression levels alter upon infection of macrophages. We attempted to further examine the expression of pseudogene and non-coding genomic region in *M. leprae*, in this study. 19 Pseudogenes, 17 non-coding genomic regions, and 21 coding genes expression in *M. leprae* maintained in the footpads of the hypertensive nude rat (SHR/NCrj-rnu) were examined by reverse transcriptase polymerase chain reaction (RT-PCR). The expression of some of these pseudogenes, non-coding genomic regions and coding genes were also examined in *M. leprae* from skin smear specimens obtained from patients with lepromatous leprosy by RT-PCR. Transcripts from pseudogenes, non-coding genomic regions and coding genes examined in this study were clearly observed in *M. leprae*. The expression patterns of some of these transcripts vary greatly among different leprosy patients. These results indicate that some of pseudogenes and non-coding genomic regions are transcribed in *M. leprae* and analysis of RNA expression patterns including pseudogene and non-coding genomic region in *M. leprae* may be useful in understanding the pathological states of infected patients.

© 2009 Elsevier Ltd. All rights reserved.

1. Introduction

Pseudogenes represent a heterogeneous collection of sequences, ranging from coding genes with an internal stop codon or frame shift mutation to extensively degraded coding genes. Bacterial pseudogenes and non-coding genomic regions were originally thought to be rare. However, a recent genomic survey identified 7000 pseudogenes in 64 bacterial genomes, a large fraction of which had arisen from "failed" horizontal gene transfers [1]. Recently evolved pathogens in particular have many pseudogenes [2], and the genomes of intracellular bacteria such as Rickettsia and Mycobacteria have exceptionally high fractions of non-coding genomic regions and pseudogenes (>25%) [3,4]. This has been accounted for by reductive genome evolution and small effective population sizes [5,6]. In addition, increased exploitation of host metabolites and reduced selection pressure for rapid growth in the nutritionally-rich eukaryotic cytoplasm may allow mutations to accumulate in essential bacterial genes [7].

The loss of genes is not necessarily associated with the loss of DNA. In fact, the half-life of a pseudogene in some eukaryotic species may be hundreds of millions of years [8]; however, it has been observed in bacteria that nonfunctional regions tend to disappear from the genome in short periods of time [9]. Several explanations have been proposed, such as that there is a systematic mutational bias toward deletion events [10] or that natural selection favors small genome sizes because of their faster replication and small metabolic cost [11].

The most striking example of reductive genome evolution may be occurring in *Mycobacterium leprae* (*M. leprae*), the causative agent of leprosy [4]. Not only is its genome small (3.3 Mb) when compared with other mycobacterial species, but it also has a small number of active genes (1600) [4] compared to closely related species (>4000) [12–15]. Strikingly, *M. leprae* contains the highest number of pseudogenes (>1000) among published genomes.

We have previously reported that some pseudogenes are expressed in *M. leprae*, and that their expression levels alter upon infection of macrophages, suggesting that some *M. leprae* pseudogenes are not just "decayed" genes, but may have functional roles in infection, intracellular parasitization and replication [16]. We also recently performed a tiling array analysis and found that in addition to many *M. leprae* coding genes, pseudogenes and non-coding genomic regions are transcribed. Our tiling array analysis showed that *M. leprae* transcripts are approximately 50% derived from coding genes, 25% from pseudogenes, and 25% from non-coding

genomic regions [17]. These results suggest that in M. leprae, many of the RNAs transcribed from pseudogenes and non-coding genomic regions may have important roles as riboregulators. In this study, to further confirm our tiling array results with regard to the expression of pseudogenes and non-coding genomic regions in M. leprae, we used RT-PCR analysis to examine the expression of 19 pseudogenes, 17 non-coding genomic regions, and 21 coding genes from M. leprae purified from the hypertensive nude rat, SHR/NCrj-rnu [18,19], and also from skin smear specimens obtained from patients with lepromatous leprosy.

2. Results

2.1. Expression of pseudogenes and non-coding genomic regions in M. leprae maintained in nude rat

M. leprae grows in SHR/NCrj-rnu rats to a higher concentration than in infected nude mice, in which only limited growth in the footpad is obtained [18,19]. Therefore, it is thought that the RNA expression profile from bacilli grown in SHR/NCrj-rnu rats would be closer to the profile of bacilli grown in humans. Our previous tiling array study demonstrated that 209 genomic region including 63 coding genes, 78 pseudogenes and 68 non-coding genomic regions were classified as strong expressers in M. leprae grown in SHR/NCrj-rnu rat [17]. Based on this tiling array study, we randomly selected 57 genomic regions including 21 coding genes, 19 pseudogenes and 17 non-coding genomic regions as highly expression region. The primer sets, which were specific for M. leprae gene and had no homology for rat or human gene, were designed for these regions to examine gene expression including pseudogene and non-coding genomic region by RT-PCR. RT-PCR analysis revealed that all the coding genes examined in this study were transcribed in M. leprae purified from SHR/NCrj-rnu nude rats (Fig. 1A upper panel). In addition, all of the examined pseudogenes (Fig. 1B upper panel) and non-coding genomic regions (Fig. 1C upper panel) were transcribed. Simultaneously, we demonstrated that no specific PCR product was detected when M. leprae RNAs without reverse transcription were used as templates (Fig. 1A–C lower panels), although some primer sets showed faint non-specific primer dimmers. These results indicate that in M. leprae, along with coding genes, some pseudogenes and non-coding genomic regions are indeed transcribed.

2.2. Pseudogenes and non-coding genomic regions expression in M. leprae obtained from lepromatous leprosy patients

To determine whether these pseudogenes and non-coding genomic regions are similarly expressed in clinical specimens, we next performed RT-PCR analysis, using several primer sets, on M. leprae RNA extracted from skin smear samples from lepromatous leprosy patients. The results show that RNA expression patterns of pseudogenes and non-coding genomic regions were quite different among patients (Fig. 2A). The pseudogene ML0043 was transcribed in specimens #3, 7, 9, and 10, whereas, ML1049 and ML1721 were only transcribed in specimens #1 and #2, and #3 and #7, respectively. The non-coding genomic region at position 39277 was transcribed in specimens #2, 7, and 8, at position 348457 transcribed in specimens #6 and 7, and at position 1450993 transcribed in specimens #7, 8, and 10. Expression of M. leprae Hsp70, which is a dominant antigen affecting the host T-cell response in leprosy, was detected in all examined specimens, indicating these specimens were infected with M. leprae. No specific PCR product was detected using primer set for Hsp70 when human specimen M. leprae RNAs not subjected to reverse transcription were used as templates (Fig. 2B), indicating that the cDNA samples from clinical
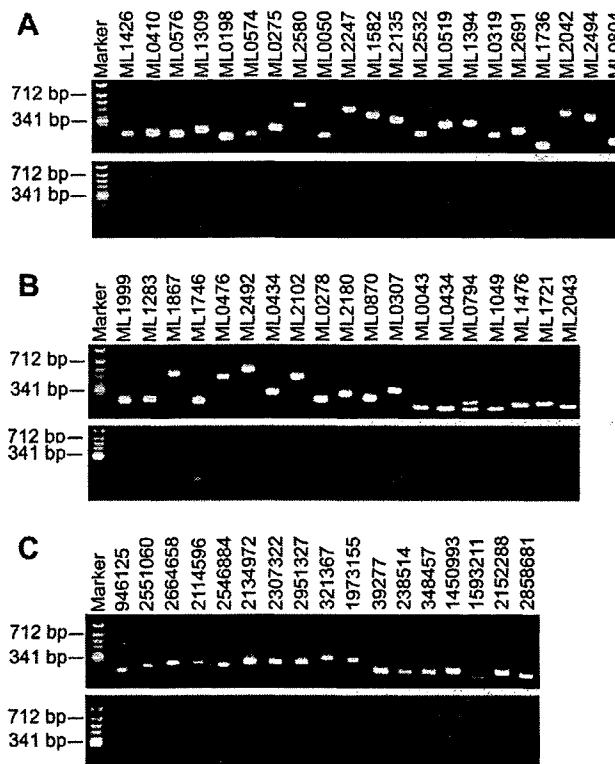

Fig. 1. RT-PCR analysis of freshly isolated M. leprae mRNA. Total RNA was isolated from freshly prepared M. leprae from SHR/NCrj-rnu footpads. After treatment with DNase, RT-PCR was performed for coding genes (A), pseudogenes (B) and non-coding genomic regions (C) as described in Materials and Methods. Bars on the left indicate DNA sizes of 712 and 341 bp. Upper panels show PCR results using cDNA and lower panels show PCR results using total RNA as template.

specimens were free from M. leprae genome. These results suggest that for some RNAs that showed similar expression levels in the SHR/NCrj-rnu hypertensive nude rat, where bacilli seem to grow under optimum conditions, expression disappears in infections of particular human subjects, or during the clinical course of infection.

3. Discussion

In this study, we demonstrated that some M. leprae pseudogenes and non-coding genomic regions are transcribed to detectable RNA levels in the SHR/NCrj-rnu nude rat and in human patients. It has been demonstrated that M. leprae has 1605 coding genes and 1116 pseudogenes. In contrast, Mycobacterium tuberculosis, which is a species closely related to M. leprae, has 3959 coding genes and only 6 pseudogenes. Thus M. leprae has exceptionally high fractions of non-coding genomic regions and pseudogenes. Pseudogenes are defined as non-functional copies or close relatives of known coding genes in which mutations, insertions, deletions and/or frame shifts have occurred. Therefore, despite having DNA sequences similar to those of normal coding genes, they are regarded as disabled copies of functional coding genes. Nevertheless, the results of this study taken together with our previous study [16,17] demonstrate that many M. leprae pseudogenes and non-coding genomic regions are transcribed.

Recently, expressed pseudogenes have been thought to be a class of non-coding RNAs (nc-RNAs) [20,21]. They act as riboregulators, which are important for both transcriptional and
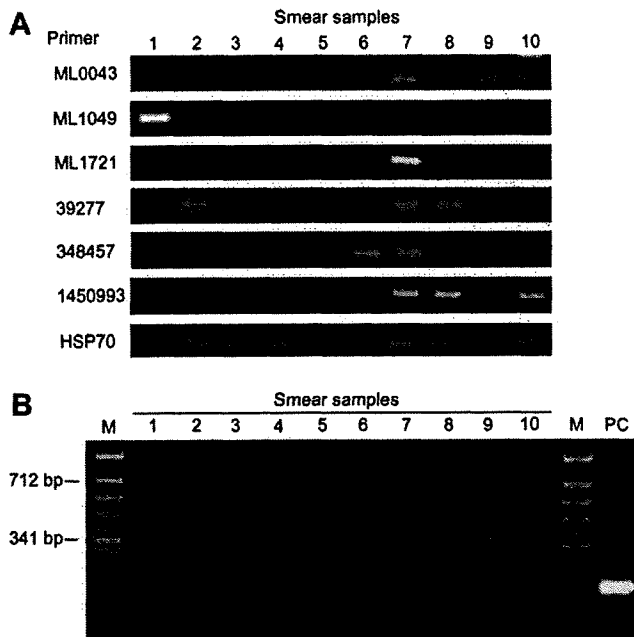
A

Smear samples

Primer   1   2   3   4   5   6   7   8   9   10

ML0043

ML1049

ML1721

39277

348457

1450993

HSP70

B

Smear samples

M   1   2   3   4   5   6   7   8   9   10   M   PC

712 bp—

341 bp—

Fig. 2. RT-PCR analysis of M. leprae RNA derived from skin smear samples from 10 lepromatous leprosy patients. Total RNA was isolated from skin smear samples. After treatment with DNase I, RT-PCR was performed for pseudogenes ML0043, ML1049, ML1721, non-coding genomic region positions 39277, 348457, 1450993, and Hsp70 as described in Materials and Methods (A). To evaluate contamination of genomic DNA, total RNAs without reverse-transcription treatment were used as template in PCR for Hsp70 (B). No specific PCR products were detected using total RNA as template. Bars on the left indicate DNA sizes of 712 and 341 bp. M: Marker, PC: positive control using cDNA of M. leprae derived from SHR/NCrj-rnu footpads as template.

posttranscriptional regulation of gene expression. As pseudogenes are functionally less constrained, they have accumulated more mutations than other coding genes. Assuming that they have functional roles in the regulation of gene expression, this property would allow more rapid functional diversification than is possible with protein-coding genes. Therefore, studies of transcribed pseudogene and non-coding genomic regions could lead to an understanding of their significance in M. leprae.

Although the roles of RNA derived from pseudogene and non-coding genomic region remain unknown in M. leprae, some of pseudogene expression has been reported in cancer and central nerve system in other species, which have antisense activities as riboregulator [22–24]. Pseudogenes also have some biological functions in processes such as cell growth and organogenesis [25]. Thus, it may be possible to speculate that some of the transcribed pseudogene and non-coding genomic region might function as riboregulators which regulate infection, intracellular parasitization and replication in M. leprae. If that is the case, it may explain why M. leprae is able to survive with only a limited number of protein-coding genes. However, further studies are needed to elucidate the possible function of transcribed pseudogenes and non-coding genomic regions in M. leprae.

Although the diagnosis of leprosy primarily relies on clinical and microscopic examination, especially in countries with high prevalence, molecular analysis provides very specific information for some unclear and/or suspected cases. Diagnosis of an isolated neural lesion, for example, can be conclusive after PCR detection of M. leprae DNA from a nerve biopsy specimen [26]. Also, RT-PCR can be used as a measure of M. leprae viability, and consequently can assess the efficacy of multidrug therapy [27]. In addition, TaqMan real-time PCR seems to be a useful tool for rapidly detecting and

quantifying M. leprae DNA in clinical specimens in which bacilli were undetectable by conventional histological staining [28].

In this study, we demonstrated that M. leprae pseudogenes and non-coding genomic regions are transcribed at different levels among leprosy patients. This evidence strongly suggests that analysis of M. leprae RNA, especially RNA transcripts derived from pseudogene and non-coding genomic regions, may be useful in understanding the pathological state of the patient. We are now conducting expanded studies utilizing large numbers of samples that include serial skin smears from the same patients during their clinical course and treatment. Results from these studies may help establish a simple diagnostic method using RT-PCR analysis of smear samples.

4. Materials and methods

4.1. Bacterial strains and growth conditions

M. leprae Thai-53 strain was amplified in footpads of hypertensive nude rats (SHR/NCrj-rnu), which were kindly provided by Dr. Y. Yogi, LRC, NIID. M. leprae was prepared as described previously [18,19]. Briefly, the feet of hypertensive nude rats (SHR/NCrj-rnu) were inoculated with bacilli, and the infected rats were maintained for 6 months. The rats were sacrificed after the infected feet became swollen. To harvest bacilli, the foot pads were collected and skin and bone removed. The tissues were then extensively homogenized in Hank's balanced salts solution (HBSS) with 0.025% Tween 80 and centrifuged at 700 × g and 4 °C for 10 min to remove tissue debris. The supernatant was treated with 0.5% trypsin at 37 °C for 1 h, followed by centrifugation at 5000 × g and 4 °C for 20 min. The supernatant was discarded and the pellet was resuspended in 10 ml HBSS with 0.025% Tween 80 and 0.25 N NaOH. A further incubation at 37 °C for 15 min was followed by another centrifugation, and the pellet was resuspended in 2 ml PBS. Two microliters of solution was spread on a glass slide and subjected to acid fast staining to count the number of bacilli.

4.2. RNA extraction from M. leprae

2.8×10^{11} bacilli were added to 2 ml RNAprotect Bacteria Reagent (QIAGEN, Germantown, MD) and were disrupted as described previously [16]. Briefly, after the addition of 0.4 ml of 1.0 mm Zirconia Beads (BioSpec Products, Bartlesville, OK) and 0.6 ml of Lysis/Binding buffer, (mirVana miRNA isolation kit; Ambion, Austin, TX), the bacilli-containing mixture was frozen and thawed and then homogenized by Micro Smash (TOMY, Tokyo, Japan) for 3 min. The freeze/thaw and Micro Smash treatments were repeated 3 times and then RNA was extracted according to mirVana miRNA isolation kit instructions. The extracted RNA (10 μg) was treated by 2U DNase I (TaKaRa, Kyoto Japan) at 37 °C for 1 hour for preventing contamination with genomic DNA.

4.3. Skin smear sampling and extraction of RNA

M. leprae from 10 lepromatous leprosy patients were collected in the same manner as is used for routine slit-skin smear testing for bacterial index examination. A surgical blade was inserted into a skin lesion and the sample with blade was immersed in 70% ethanol and stored at room temperature. The ethanol-containing samples were centrifuged at 20,000 × g for 1 min, and then 350 μl of Buffer RLT (RNeasy Mini Kit; QIAGEN) was added to the pellet. The samples were then treated by 4 freeze/thaw cycles and subsequently centrifuged at 20,000 × g for 5 min. RNA extraction was performed using the RNAeasy mini kit according to the manufacturer's protocol. The extracted RNA (10 μg) was treated by

2U DNase I (TaKaRa, Kyoto Japan) at 37 °C for 1 hour for preventing contamination with genomic DNA.

4.4. Reverse transcription and polymerase chain reaction (RT-PCR)

Highly expressed coding genomic, pseudogenomic and non-coding genomic regions determined from our tiling array results [17] were chosen for RT-PCR analysis. Reverse transcription was performed using High-Capacity cDNA Reverse Transcription Kits (Applied Biosystems, Foster City, CA) according to the manufacturer's protocol. The primer sequences are shown in the Table 1, and 5′-ACTAGCGGTATCGATCTGAC-3′ and

5′-GTGATGCGTTGGAATTCGG-3′ for Hsp70 (ML2496) to detect the presence of M. leprae. Touchdown PCR conditions were described previously [29].

Acknowledgments

Table 1
Primer sequence designed and used for RT-PCR.

	PCR target	Product length	Forward primer (5′-3′)	Reverse primer (5′-3′)
Gene	ML1426	207	CTGATCAGGACGGTCGGTAT	TCTGGCTTCGGTCTCAGTCT
	ML0410	214	CAGATTGGAGCGCATTACCT	ATAATCACCTGCGGCATCTT
	ML0576	206	TGGCGTCTGGTGTCAATATC	CCAGCATAGTCGAGTCACAGG
	ML1309	247	GACCTTCGAGGATCTGTTCG	ATAGACGTCATCGAGCGACA
	ML0198	186	GAACTGTGAAGTGGTTCAACG	AGCGAACTCCAGTGGCTTG
	ML0574	205	TTGCTAGTACGGCAACCAGA	TGTTGAACAGGACGGTATGG
	ML0275	263	AAGAACACCGCTTGAGTTGG	ATGTTCGAGGAACGGTTACG
	ML2580	563	CATCAACACCATGAGCATCC	TCTACCTGGCGTTGCCTATC
	ML0050	194	TCATCGTCGGTCTTGGTGTA	CTCAGCCAAGAACGGAACTT
	ML2247	511	GGCACCTTCACCAACCTAGA	CCAACTTAGGATCCGCTTGA
	ML1582	420	AGCTTGGTCGGTATGGTGAC	TGCTTGTGTAGCATCGGAAC
	ML2135	367	GAACATCATCGTGTGGTTGC	CGATGACACCGACTATGTGG
	ML2532	212	GTAAGTCGACGCAGCCGTAG	TGATGCGCAGCCAGATTA
	ML0519	318	AACAGCTGTCGGCTCTGATT	CAAGCAGGTAGCCTTGGACT
	ML1394	334	GTACGGATCGAGGATGCACT	GTCGCTGCAGTAATCGGTAA
	ML0319	213	TGTCCAGCCTTCTCGAAGTT	GTCCATCACCAGTGACATCG
	ML2691	259	CAGCGAGCTGGTAACTGACA	CAGTTCGTTGAGCCACTTGA
	ML1736	133	CAACGCCATCACGTAGTCAC	CATCACCGTGTACACCAAGC
	ML2042	451	AAGTGGCGCGTAGTGTTCTT	AGGCTGACGTCTTGAGCAAT
	ML2494	408	ATCCGTTGTCCATCTTCGAC	CAACATCGGTGACTTGTTCG
	ML0804	169	CGCTCGTCTTCACTCATGC	AGGATCCGGAGCTGTTCTTC
Pseudogene	ML1999	229	GATGCTGACATCGGCTACG	GCATCAATGCGACCAAGTTA
	ML1283	234	ACCTACCGCTGTTGACCATC	TGTAGCCATTGAGCACTTCG
	ML1867	522	ACCATCGCCGTGATCTTATC	TGCAAGACTCTGGTCATTCG
	ML1746	220	GAAGGTCTCGGTGGTGTGTT	CAACCGACTCATGTTGAACG
	ML0476	465	TCGCAACTTCACTGATCGTC	GTCTGGCACCAATACCGAGT
	ML2492	578	GGCTGGTCTGATGGTATCGT	GCGCGACATATTCACAGAGA
	ML0434	275	CGTGTCGGTAGTCCTTCCAT	AGCGAATCAACTGGAACACC
	ML2102	486	GCACATATGGTGCACACCTC	CCATTGGCTACAGGATACGG
	ML0278	215	GGCTGTCCGAATCATATTGC	GAGTCCACACACAACGATGAA
	ML2180	275	GGAATAGGCTTGTTGCCGTGT	ATCATCCGGCTAGGAGCTG
	ML0870	239	GCAGGAGGAACTGGATTCAA	GTCCGATGTCTCGATGTCCT
	ML0307	333	AGTACAGCGTAGCGGTCAGC	TGACTTCCTGTGGCAATGAG
	ML0043	199	GCATTCTCGAGACAGTGCAA	TGGCCATGTCATCACTAGGA
	ML0434	201	TGGAACACCTCGTCGTATGTGG	TATAAGTGGCACCGCCGAACTC
	ML0794	191	AAAGACGGAGACTACGATG	GTTTAGAAGGTTGGTCGTTG
	ML1049	186	GCCTGCTAATTCTTGTCGATG	TCAGCGTGGATCAGAACTC
	ML1476	223	CGCCAGTAATCGTGTTGTCTG	TTGCCGCTTCCAATCCATC
	ML1721	233	TGTGCTCAAGTTCTTCCGT	GAGTCAAGGCTGATAGAAGGT
	ML2043	200	TCAACATGGCGATCTGCATTC	TGCGTGACCTTACAACGCT
Non-coding region	946125	156	GCGCCAAGGTATGAAGAACA	TTAGCGGATCCTCCTCGTAG
	2551060	194	ACATTCGAGACCAGCTACCG	TTCCGCTTGGAGGATAATTG
	2664658	227	TGACCTTGCCGATTACGATT	GCCATTGAACTGGCCATC
	2114596	225	AGCCACACTGCACTTCACAC	TTCGCTAGTGTTGTGTGTTGG
	2546884	202	TCAATATGGCTTCCTATGTTGC	GCTGCATTAATCCATGATTCG
	2134972	242	CGGAATCCTGTTGACGTGTT	CGGCGCTAACAACTATCCTC
	2307322	242	GGTTCACCGGAAGAGTTGG	CGCGACGACTAAGCCAGTAG
	2951327	247	GTCTGTCCTGCGTTCTTGGT	ATCTAGCTTCGGAGGCATCA
	321367	299	GCAGCAATGGATAGCTGACA	AATCGATGTTGGTGGTTGGT
	1973155	276	GACGCTGAAGATGGTCGATT	GACGCTGAAGATGGTCGATT
	39277	180	TGAAGGCGATATCGATGCAG	ATGGTGCAAGGGATAACATCAG
	238514	191	TGCCGATGATTACATCATCC	CATCGAGTCCAAGCTCAAC
	348457	202	TGGACTCGATGTTGAAGTG	TGCTTAGCTATGCAGTGAG
	1450993	224	TGCGCTAGAAGGTTGCCCGTATG	TCAATGTGGCCGCACCTGAA
	1593211	191	CATCGAGTCCAAGCTCAAC	TGCCGATGATTACATCATCC
	2152288	241	CCGATATGTTCGGTAGTCGT	GCATCGATATCGCCTTCAG
	2858681	217	ATGTTGGTTGAGCTTGGAC	TTGCTTAGCTATGCAGTGAG

References

[1] Liu Y, Harrison PM, Kunin V, Gerstein M. Comprehensive analysis of pseudogenes in prokaryotes: widespread gene decay and failure of putative horizontally transferred genes. Genome Biol 2004;5:R64.

[2] Lerat E, Ochman H. Recognizing the pseudogenes in bacterial genomes. Nucleic Acids Res 2005;33:3125–32.

[3] Andersson SG, Zomorodipour A, Andersson JO, Sicheritz-Ponten T, Alsmark UC, Podowski RM, et al. The genome sequence of *Rickettsia prowazekii* and the origin of mitochondria. Nature 1998;396:133–40.

[4] Cole ST, Eiglmeier K, Parkhill J, James KD, Thomson NR, Wheeler PR, et al. Massive gene decay in the leprosy bacillus. Nature 2001;409:1007–11.

[5] Andersson SG, Kurland CG. Reductive evolution of resident genomes. Trends Microbiol 1998;6:263–8.

[6] Darby AC, Cho NH, Fuxelius HH, Westberg J, Andersson SG. Intracellular pathogens go extreme: genome evolution in the Rickettsiales. Trends Genet 2007;23:511–20.

[7] Lawrence JG, Hendrix RW, Casjens S. Where are the pseudogenes in bacterial genomes? Trends Microbiol 2001;9:535–40.

[8] Graur D, Shuali Y, Li WH. Deletions in processed pseudogenes accumulate faster in rodents than in humans. J Mol Evol 1989;28:279–85.

[9] Gomez-Valero L, Latorre A, Silva FJ. The evolutionary fate of nonfunctional DNA in the bacterial endosymbiont *Buchnera aphidicola*. Mol Biol Evol 2004;21:2172–81.

[10] Mira A, Ochman H, Moran NA. Deletional bias and the evolution of bacterial genomes. Trends Genet 2001;17:589–96.

[11] Cavalier-Smith T. Economy, speed and size matter: evolutionary forces driving nuclear genome miniaturization and expansion. Ann Bot (Lond) 2005;95:147–75.

[12] Cole ST, Brosch R, Parkhill J, Garnier T, Churcher C, Harris D, et al. Deciphering the biology of *Mycobacterium tuberculosis* from the complete genome sequence. Nature 1998;393:537–44.

[13] Fleischmann RD, Alland D, Eisen JA, Carpenter L, White O, Peterson J, et al. Whole-genome comparison of *Mycobacterium tuberculosis* clinical and laboratory strains. J Bacteriol 2002;184:5479–90.

[14] Garnier T, Eiglmeier K, Camus JC, Medina N, Mansoor H, Pryor M, et al. The complete genome sequence of *Mycobacterium bovis*. Proc Natl Acad Sci U S A 2003;100:7877–82.

[15] Li L, Bannantine JP, Zhang Q, Amonsin A, May BJ, Alt D, et al. The complete genome sequence of *Mycobacterium avium* subspecies *paratuberculosis*. Proc Natl Acad Sci U S A 2005;102:12344–9.

[16] Suzuki K, Nakata N, Bang PD, Ishii N, Makino M. High-level expression of pseudogenes in *Mycobacterium leprae*. FEMS Microbiol Lett 2006;259:208–14.

[17] Akama T, Suzuki K, Tanigawa K, Kawashima A, Wu H, Nakata N, et al. Whole genome tiling array analysis of *Mycobacterium leprae* RNA reveals high expression of pseudogenes and non-coding regions. J Bacteriol 2009;191:3321–7.

[18] Yogi Y, Banba T, Kobayashi M, Katoh H, Jahan N, Endoh M, et al. Leprosy in hypertensive nude rats (SHR/NCrj-rnu). Int J Lepr Other Mycobact Dis 1999;67:435–45.

[19] Yogi Y, Endoh M, Banba T, Kobayashi M, Katoh H, Suzuki K, et al. Susceptibility to *Mycobacterium leprae* of congenic hypertensive nude rat (SHR/NCrj-rnu) and production of cytokine from the resident peritoneal macrophages. Jpn J Lepr 2002;71:39–45.

[20] Eddy SR. Non-coding RNA genes and the modern RNA world. Nat Rev Genet 2001;2:919–29.

[21] Erdmann VA, Barciszewska MZ, Hochberg A, de Groot N, Barciszewski J. Regulatory RNAs. Cell Mol Life Sci 2001;58:960–77.

[22] Korneev SA, Park JH, O'Shea M. Neuronal expression of neural nitric oxide synthase (nNOS) protein is suppressed by an antisense RNA transcribed from an NOS pseudogene. J Neurosci 1999;19:7711–20.

[23] Lu W, Zhou D, Glusman G, Utleg AG, White JT, Nelson PS, et al. KLK31P is a novel androgen regulated and transcribed pseudogene of kallikreins that is expressed at lower levels in prostate cancer cells than in normal prostate cells. Prostate 2006;66:936–44.

[24] Suo G, Han J, Wang X, Zhang J, Zhao Y, Dai J. Oct4 pseudogenes are transcribed in cancers. Biochem Biophys Res Commun 2005;337:1047–51.

[25] Kandouz M, Bier A, Carystinos GD, Alaoui-Jamali MA, Batist G. Connexin43 pseudogene is expressed in tumor cells and inhibits growth. Oncogene 2004;23:4763–70.

[26] Jardim MR, Antunes SL, Santos AR, Nascimento OJ, Nery JA, Sales AM, et al. Criteria for diagnosis of pure neural leprosy. J Neurol 2003;250:806–9.

[27] Chae GT, Kim MJ, Kang TJ, Lee SB, Shin HK, Kim JP, et al. DNA-PCR and RT-PCR for the 18-kDa gene of *Mycobacterium leprae* to assess the efficacy of multidrug therapy for leprosy. J Med Microbiol 2002;51:417–22.

[28] Martinez AN, Britto CF, Nery JA, Sampaio EP, Jardim MR, Sarno EN, et al. Evaluation of real-time and conventional PCR targeting complex 85 genes for detection of *Mycobacterium leprae* DNA in skin biopsy samples from patients diagnosed with leprosy. J Clin Microbiol 2006;44:3154–9.

[29] Suzuki K, Yanagi M, Mori-Aoki A, Moriyama E, Ishii KJ, Kohn LD. Transfection of single-stranded hepatitis A virus RNA activates MHC class I pathway. Clin Exp Immunol 2002;127:234–42.

ORIGINAL ARTICLE

Evaluation of polymerase chain reaction-based detection of *Mycobacterium leprae* for the diagnosis of leprosy

Pham Dang BANG,[1,2] Koichi SUZUKI,[3] Le Thi PHUONG,[2] Tran Man CHU,[2] Norihisa ISHII,[3] Tran Hau KHANG[1,2]

[1]Dermatology Department, Hanoi Medical University, [2]National Institute of Dermato-Venereology, Dong Da District, Hanoi, Vietnam, and [3]Department of Bioregulation, Leprosy Research Center, National Institute of Infectious Diseases, Tokyo, Japan

ABSTRACT

Because *Mycobacterium leprae* cannot be cultivated *in vitro*, laboratory diagnosis of leprosy is generally made by microscopic and histopathological examination. The objective of the present study was to evaluate the sensitivity and utility of polymerase chain reaction (PCR) to detect *M. leprae* in comparison with other conventional methods for diagnosis such as split skin smears, histopathology and serodiagnosis. PCR amplification of the *M. leprae*-specific 16S ribosomal RNA was compared to other methods. Samples included 37 multibacillary (MB) patients with a positive bacteriological index (BI), 32 newly diagnosed paucibacillary (PB) patients whose BI were negative and 30 plaque psoriasis patients not residing in leprosy endemic areas as controls. The sensitivity of PCR was 30 fg of *M. leprae* DNA, which is equivalent to the DNA from 8.3 bacilli. The detection rate in MB and PB were 100% and 50%, respectively; the specificity was 100%. Semiquantitative evaluation of PCR correlated well with BI, but not with the morphological index (MI) nor with the serum antibody against phenolic glycolipid-1 (PGL-1). PCR detection of *M. leprae* targeting 16S ribosomal RNA was specific and more sensitive than conventional methods, and can contribute to early and accurate diagnosis of leprosy.

Key words: leprosy, *Mycobacterium leprae*, polymerase chain reaction.

INTRODUCTION

Leprosy is a chronic infectious disease where delay in diagnosis and treatment can lead to deformities, disabilities and social stigma for the rest of a patient's life. Despite being one of the earliest bacteria identified under the microscope, *Mycobacterium leprae*, the causative pathogen for leprosy, cannot be cultivated *in vitro*. Therefore, classical bacteriological methods to identify pathogenic bacteria cannot be applied for the diagnosis of leprosy. The differential diagnosis of leprosy has been performed based on clinical criteria and the presence of acid-fast bacilli (AFB) from tissue smears or tissue sections stained by Ziehl–Neelsen or Fite–Faraco methods. Non-polymerase chain reaction (PCR)-based detection of *M. leprae* DNA requires at least 10^4 organisms/g tissue in order to obtain reliable results.[1] Therefore, these methods are not routinely used as a diagnostic tool to detect *M. leprae*, particularly in patients with an indeterminate type at the tuberculoid end of the leprosy spectrum where AFB are generally rare or virtually absent.[2] This situation makes definitive and differential diagnosis difficult, especially in cases of paucibacillary (PB) patients and patients being monitored for possible relapse after completing multidrug therapy (MDT) led by the World Health Organization (WHO).

In the last two decades, new molecular biology methods, PCR amplification, have been developed

269

as reliable and sensitive diagnostic tools for the detection of pathogens for many infectious diseases including leprosy.[3,4] Several investigators have used PCR to amplify various genomic sequences of *M. leprae* in order to improve detection of low numbers of bacteria.[5-10] In Vietnam, PCR has also been applied for the diagnosis of some communicable diseases other than leprosy.[11-13] Ideally, sensitive and specific methods such as PCR provide a promising approach for early diagnosis and treatment, leading to possible reduction of permanent deformities and disabilities, and a reduced socioeconomic burden due to leprosy in endemic countries.

In this study, we evaluated the usefulness of PCR analysis by comparing with other conventional methods, such as slit-skin smear, histopathological study and phenolic glycolipid-1 (PGL-1)-based serodiagnosis.

METHODS

Patients

Sixty-nine leprosy patients attending the National Institute of Dermato-Venereology, Da Nang Dermatology Hospital and Quy Hoa Central Leprosy-Dermatology Hospital in Vietnam between February and October 2004 were included in this study. These patients were divided into two groups: (i) 37 multibacillary (MB) patients with distinctive histopathological lesions typical of leprosy and a positive bacteriological index (BI) either newly diagnosed or being treated with WHO's MDT regimen; and (ii) 32 PB patients having a negative BI but distinctive histopathological lesions before receiving MDT. The MDT regimen used in MB patients was a combination of 600 mg rifampicin monthly, 300 mg clofazimine monthly, 50 mg clofazimine daily and 100 mg dapsone daily for a total of 12 months. Average ages in each group were 32.5 years (range, 10–76) and 33.4 years (range, 11–76), respectively. Forty-seven of 69 patients were men (23 MB and 24 PB) and 22 were women (14 MB and eight PB). The male : female ratio in this research was similar to annually reported data in Vietnam (unpubl. data from National Institute of Dermato-Venereology, Hanoi, Vietnam, "Leprosy Elimination Program Report from 1995–2004", 2005 in Vietnamese). Thirty plaque psoriasis patients hospitalized in the National Insti-

tute of Dermato-Venereology during the same period were selected as a control group, of whom 21 were men and nine were women with an average age of 51.3 years (range, 15–81). The study was approved by the Ethics Committee of the National Institute of Dermato-Venereology. Each patient signed a written informed consent prior to specimen collection.

Slit-skin smear and biopsies

Slit-skin smears and 4-mm punch biopsies were obtained from two adjacent positions on the border of the most active lesion found in each patient according to standard procedures. Slit-skin smears were also taken from both ear lobes. All smears were prepared on microscopic slides, stained by the classic Ziehl–Neelsen method and observed by well-trained technicians to identify AFB. BI and morphological index (MI) were evaluated according to Ridley's logarithmic scale.[14] BI of a patient is the mean of BI at all skin smear samples in his/her body. MI is the percentage of solid bacilli in the samples. Each biopsy sample was divided into two equal parts: one half was fixed in 4% (v/v) buffered neutral formalin (Sigma, Saint Louis, MO, USA) and then dehydrated in a graded series of ethanol (Sigma) and embedded in paraffin. Sections were stained by two methods: hematoxylin–eosin staining for histopathological examination and Fite–Faraco staining for the detection of AFB. The other half of the biopsy sample was frozen at –80°C for use in the PCR study. The results of skin smears and histopathological evaluations were used as criteria for grouping the patients as described above.

Serological examination of anti-PGL-1 antibody

A 5-mL venous blood sample was collected by venipuncture from each patient. Samples were centrifuged and serum was separated and kept frozen at –40°C until processed. Serum samples were tested for the presence of immunoglobulin (Ig)M anti-PGL-1 antibody using a *M. leprae* Particle Agglutination (MLPA) kit (Fujirebio, Tokyo, Japan) according to the manufacturer's procedures as described.[15] Briefly, three drops (75 µL) of serum diluent were added into the first well and one drop (25 µL) of the same diluent was added to the second and the third well of a 96-well U-type microdiluent plate. Test serum (25 µL) was added to the first well then mixed by pipetting, and the same volume of

diluted serum was serially transferred from the first to the second well and from the second to the third well. Diluted serum (25 mL) in the third well was discarded. One drop of unsensitized (without antigen) control particles and one drop of sensitized (antigen-bound) particles were then added to the second and the third wells, respectively. After being mixed briefly with the microplate mixer, the plate was incubated at 37°C for 1 h. The test was interpreted with the naked eye as negative if the sensitized particles formed a definite compact button with a smooth round outer margin. The result was regarded as positive if these particles formed one of the following: (i) a compact ring with smooth round outer margin; (ii) a significantly large ring with rough outer margin with agglutination in the periphery; or (iii) a filmy mat of homogeneous agglutination covering the entire bottom of the well.

DNA extraction

The frozen part of each skin biopsy specimen was incised into small pieces with sterile scissors and placed in a 1.5-mL sterile centrifuge tube containing 360 μL TE buffer (10 mmol/M Tris-Cl, pH 7.5 and 1 mmol/L ethylenediaminetetraacetic acid) (Bio-Rad, Hercules, CA, USA). Forty microliters of proteinase K (10 mg/mL) (Qiagen, Hilden, Germany) was added to the tube. The mixture was covered with mineral oil to prevent evaporation, incubated at 55°C for 18 h and at 97°C for 10 min to inactivate proteinase K. DNA was then extracted with an equal volume of phenol/chloroform/isoamyl alcohol (25:24:1) mixture (Bio-Rad). After separation by centrifugation for 5 min at 12 000 g, the DNA in the upper aqueous phase was precipitated with absolute ethanol and sodium acetate (Sigma). The DNA pellet was washed twice with 70% ethanol (Sigma), dissolved in 100 μL of TE buffer (Bio-Rad) and stored at –20°C until use. Purified *M. leprae* DNA as a positive control, obtained from experimentally infected mouse foot pads, purified *Mycobacterium smegmatis* DNA and purified *Escherichia coli* DNA were kindly provided by Dr Yasuko Yogi, Leprosy Research Center, National Institute of Infectious Diseases, Tokyo, Japan.

PCR amplification

Primers P1, P2 and P3 employed in this study were previously published.[16,17] Primers P1 (5′-AGA GTT TGA TCC TGG CTC AG-3′) and P2 (5′-CGG AAA GGT CTC TAA AAA ATC TT-3′) served as forward primers whereas primer P3 (5′-CAT CCT GCA CCG CAA AAA GCT T-3′) was a reverse primer. These primers were synthesized by Invitrogen (Tokyo, Japan). P1–P3 primers amplify a 231-bp fragment of 16S ribosomal RNA coding gene of all Mycobacterium species,[18] while P2–P3 primers amplify a 172-bp fragment of the same gene, but more specific for *M. leprae* because primer P2 was designed to be a unique nucleotide sequence among these species. DNA solution (5 μL) extracted from a tissue specimen or purified *M. leprae* DNA (positive control) or sterile TE buffer (negative control) was added to the cocktail of amplification to a total amount of 50 μL containing 0.5 μM of each primer, 0.2 mmol/L of each dNTP (dATP, dCTP, dGTP and dTTP) (Bio-Rad), 1 IU of Taq DNA polymerase (Qiagen), 5 μL of 10X PCR buffer (200 mmol/L Tris-HCl pH 8.4, 500 mmol/L KCl), and 1.5 mmol/L $MgCl_2$ (Bio-Rad). Our unpublished experiment found that a $MgCl_2$ concentration of 1.5 mmol/L gave the best results in this PCR protocol. The PCR was performed in a Bio-Rad automated Thermal Cycler (iCycler model) with an initial denaturation step at 95°C for 3 min followed by 40 cycles (denaturation at 95°C for 20 s, annealing at 55°C for 20 s and elongation at 72°C for 30 s) and a final extension at 72°C for 5 min. The amplified product was detected by electrophoresis on a 1.5% agarose gel (Bio-Rad). The DNA was stained with ethidium bromide and visualized on a 302-nm ultraviolet transiluminator (Bio-Rad). The PCR results were determined by the presence or absence of the specific DNA band. The results were further semiquantified as weak positive (1+) or strong positive (2+) according to the brightness of the amplified DNA band by comparison with the control positive band amplified from 0.1 μg purified *M. leprae* DNA.

RESULTS

Sensitivity and specificity of PCR

We first evaluated the specificity of the PCR method using two different primer sets. The amplifications using primers P1–P3 were universal to all mycobacterial species, whereas amplification using P2–P3 was specific to *M. leprae.* To test the specificity, we
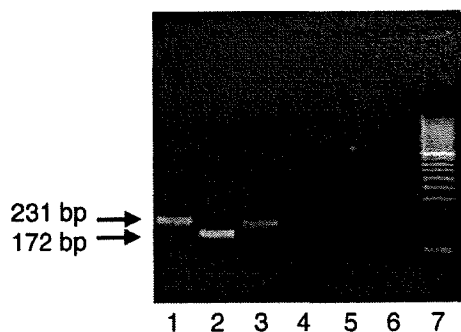
Figure 1. Specificity of polymerase chain reaction (PCR) primers to detect *Mycobacterium leprae*. Purified DNA from *M. leprae*, *Mycobacterium smegmatis* and *Escherichia coli* were subjected to PCR amplification using primer pairs P1–P3 or P2–P3 as described in Methods. Samples were analyzed by 1.5% agarose gel electrophoresis and specific 231-bp (primers P1–P3) and 172-bp (primers P2–P3) DNA was visualized under ultraviolet light by ethidium bromide staining. Lanes 1 and 2 for *M. leprae* DNA, lanes 3 and 4 for *M. smegmatis* DNA, lanes 5 and 6 for *E. coli* DNA, and lane 7 for 100-bp DNA ladder. Primers P1–P3 were used for lanes 1, 3 and 5, and primers P2–P3 for lanes 2, 4 and 6.

Figure 2. Determination of end-point detection limit of *Mycobacterium leprae* DNA by polymerase chain reaction (PCR). Purified *M. leprae* DNA was serially diluted and subjected to PCR amplification using primers P2–P3 as described in Methods. Samples were analyzed by 1.5% agarose gel electrophoresis and specific 172-bp DNA was visualized under ultraviolet light by ethidium bromide staining. Lanes 2–7: *M. leprae* DNA equivalent to 300 pg, 30 pg, 3 pg, 300 fg, 30 fg and 3 fg, respectively. Lanes 1 and 8: the 100-bp DNA ladder.

utilized DNA from *M. leprae*, *M. smegmatis* and *E. coli* as PCR templates. As expected, primers P1–P3 detected DNA from *M. leprae* and *M. smegmatis* as a specific 231-bp band (Fig. 1, lanes 1 and 3, respectively). Also as expected, primers P2–P3 detected only *M. leprae* as a specific 172-bp band, but not *M. smegmatis* (Fig. 1, lanes 2 and 4, respectively). Neither primer pair amplified *E. coli* DNA (Fig. 1, lanes 5 and 6). These results indicate that the PCR protocol and primers employed in the present study provide reliable evidence to detect *M. leprae* DNA.

We next evaluated the detection limitation by the PCR protocol employed in this study using serial 10-fold dilution of purified *M. leprae* DNA as templates. *M. leprae* genomic DNA (300 pg to 3 fg) were amplified under the conditions described in Methods using P2–P3 primers. As shown in Figure 2, the amount of final PCR product corresponded well with the amount of template *M. leprae* DNA used. The result suggests that it is possible to estimate the amount of template DNA based on the brightness of the specific band on agarose gel in the conditions used in this study. The amplified PCR products were
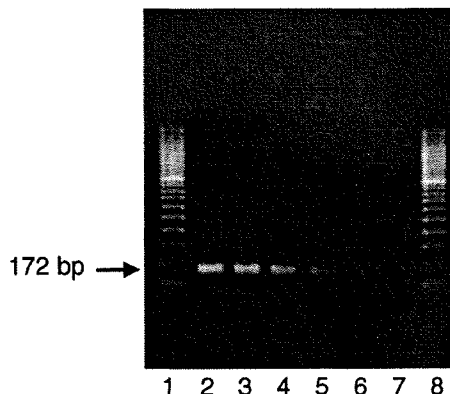
detectable at 30 fg (Fig. 2, lane 6), but not at 3 fg (Fig. 2, lane 7) of *M. leprae* DNA. Given that the size of the *M. leprae* genome is 3.27 Mb corresponding to a weight of 3.6 fg,[19] we estimate that our PCR protocol was able to detect *M. leprae* DNA from at least 8.3 bacilli.

Comparison of PCR with other conventional methods for the diagnosis of leprosy

Typical results of PCR on clinical samples, which supposedly had different amounts of *M. leprae* as indicated by BI values determined from Fite–Faraco staining, are shown in Figure 3. The sample having the highest BI gave the strongest PCR amplification (Figure 3, lanes 2–13), and the PCR results correlated well with BI evaluated by microscopic examination. Of note, PCR was also positive in half of the samples even though their BI were evaluated as zero; that is, acid fast bacilli had not been detected by Fite–Faraco staining of skin smear samples. The overall results of semiquantitative evaluation of PCR for all the samples with their clinical classification and BI values based on microscopic examination of slit-skin smear samples are summarized in Table 1. All the MB samples were positive for PCR detection of